

Review

Assessment of Machine Learning Techniques for Simulating Reacting Flow: From Plasma-Assisted Ignition to Turbulent Flame Propagation

Mashrur Ertija Shejan, Sharif Md Yousuf Bhuiyan, Marco P. Schoen * and Rajib Mahamud *

Department of Mechanical Engineering, Idaho State University, Colonial Hall, Room 102, Pocatello, ID 83209, USA; mashrurshejan@isu.edu (M.E.S.); sharifmdyousufbhu@isu.edu (S.M.Y.B.)

* Correspondence: marcoschoen@isu.edu (M.P.S.); rajibmahamud@isu.edu (R.M.)

Abstract: Combustion involves the study of multiphysics phenomena that includes fluid and chemical kinetics, chemical reactions and complex nonlinear processes across various time and space scales. Accurate simulation of combustion is essential for designing energy conversion systems. Nonetheless, due to its multiscale, multiphysics nature, simulating these systems at full resolution is typically difficult. The massive and complex data generated from experiments and simulations, particularly in turbulent combustion, presents both a challenge and a research opportunity for advancing combustion studies. Machine learning facilitates data-driven techniques to manage the substantial amount of combustion data that is either obtained through experiments or simulations, and thereby can find the hidden patterns underlying these data. Alternatively, machine learning models can be useful to make predictions with comparable accuracy to existing models, while reducing computational costs significantly. In this era of big data, machine learning is rapidly evolving, offering promising opportunities to explore its integration with combustion research. This work provides an in-depth overview of machine learning applications in turbulent combustion modeling and presents the application of machine learning models: Decision Trees (DT) and Random Forests (RF), for the spatio-temporal prediction of plasma-assisted ignition kernels, based on the initial degree of ionization, with model validations against DNS data. The results demonstrate that properly trained machine learning models can accurately predict the spatio-temporal ignition kernel profile based on the initial energy deposition and distribution.

Keywords: machine learning; combustion; plasma; ignition; turbulence; DNS; DT; RF



Citation: Shejan, M.E.; Bhuiyan, S.M.Y.; Schoen, M.P.; Mahamud, R. Assessment of Machine Learning Techniques for Simulating Reacting Flow: From Plasma-Assisted Ignition to Turbulent Flame Propagation. *Energies* **2024**, *17*, 4887. <https://doi.org/10.3390/en17194887>

Academic Editor: Andrey A. Kurkin

Received: 30 July 2024

Revised: 24 September 2024

Accepted: 25 September 2024

Published: 29 September 2024



Copyright: © 2024 by the authors. Licensee MDPI, Basel, Switzerland. This article is an open access article distributed under the terms and conditions of the Creative Commons Attribution (CC BY) license (<https://creativecommons.org/licenses/by/4.0/>).

1. Introduction

Combustion is a complex chemical process, comprising multiple stages (Figure 1) that depend on the properties of combustible materials. It is an essential chemical event that may be considered the ultimate step in the oxidation process of certain compounds. In addition to the core chemical reactions, combustion involves physical processes such as the transfer of mass and energy through diffusion and convection. These mechanisms are crucial for the distribution of reactants and continuous reaction across both time and space scales [1]. Aspects of fluid dynamics, turbulent and molecular transport [2], and chemistry are closely interconnected in combustion mechanisms that affect the entire process from the flame stability to its behavior [3].

Turbulent combustion is the result of many highly nonlinear and multiscale phenomena with numerous chemical reactions involving hundreds of species, their molecular and turbulent transport, radiative and convective heat transfer, strong density variations, etc. Turbulent combustion in gaseous systems can lead to sudden detonation. This phenomenon can be strongly influenced by geometric parameters, affecting detonation wave behavior and the overall performance of a combustion system [4–8]. Managing this phase is crucial for ensuring safety and stability during high-energy transitions [9]. Consequently,

the combustion of solid material involves pyrolysis that produces volatile gases through thermal decomposition and contributes to flame propagation [10,11]. In this process, turbulent transfer significantly dominates the molecular transfer [12] through accelerating the mixing of gases and the distribution of heat. Depending on the local conditions, different phenomena contribute differently to the main variables of interest, such as heat release rate, combustion stability, etc.

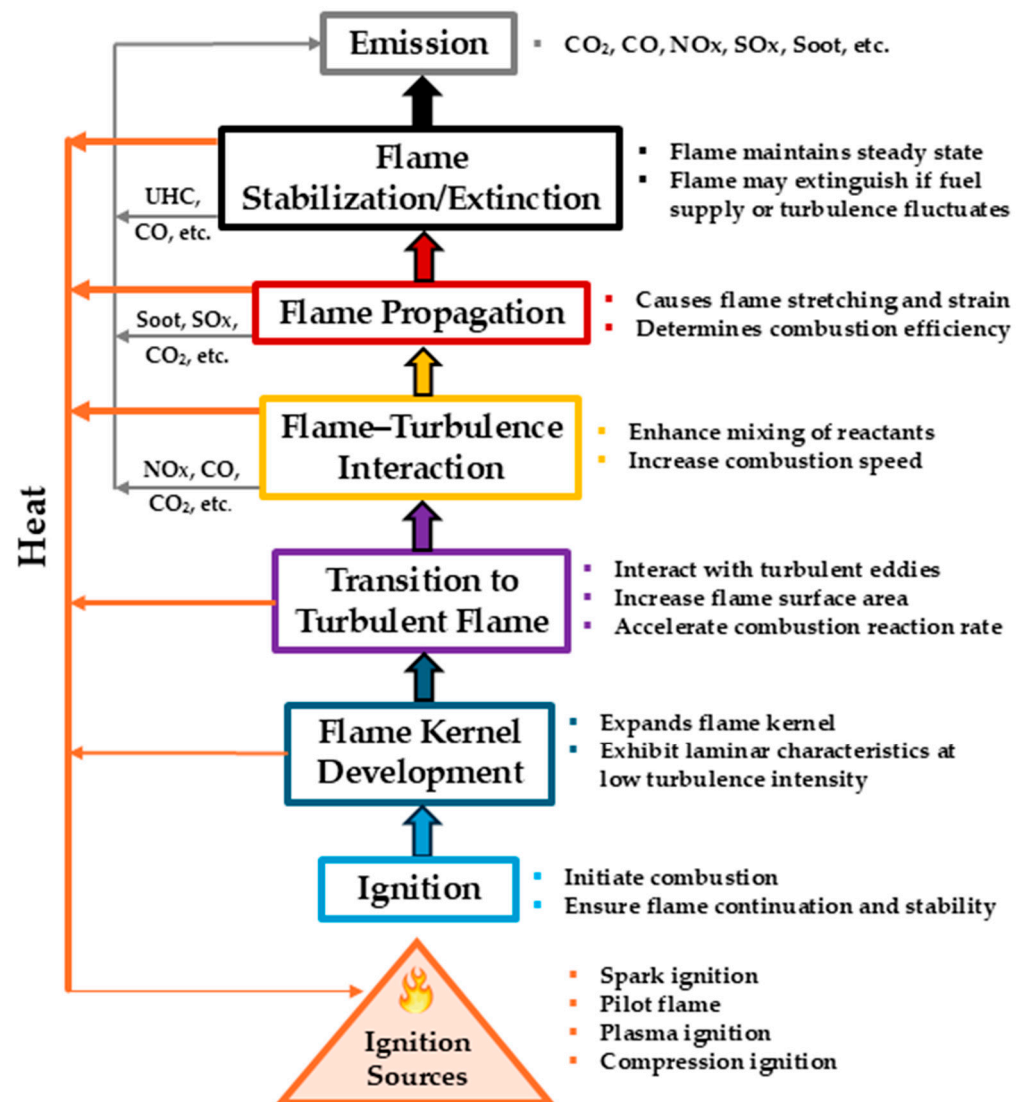


Figure 1. Combustion process pathways: from ignition to emission.

Almost all the practical combustion systems, including those in energy generation, aerospace, and combustion engines heavily rely on turbulent combustion. It plays a pivotal role in various industrial applications, energy production, and environmental processes [13]. Therefore, understanding combustion, particularly turbulent combustion, is crucial for optimizing combustion systems and minimizing their environmental impact. However, the knowledge of turbulent combustion processes remains incomplete, especially the interaction between rapid oxidative chemical reactions, strong heat and mass transport fluxes, and intense fluid-mechanical turbulence [14,15] (Figure 2).

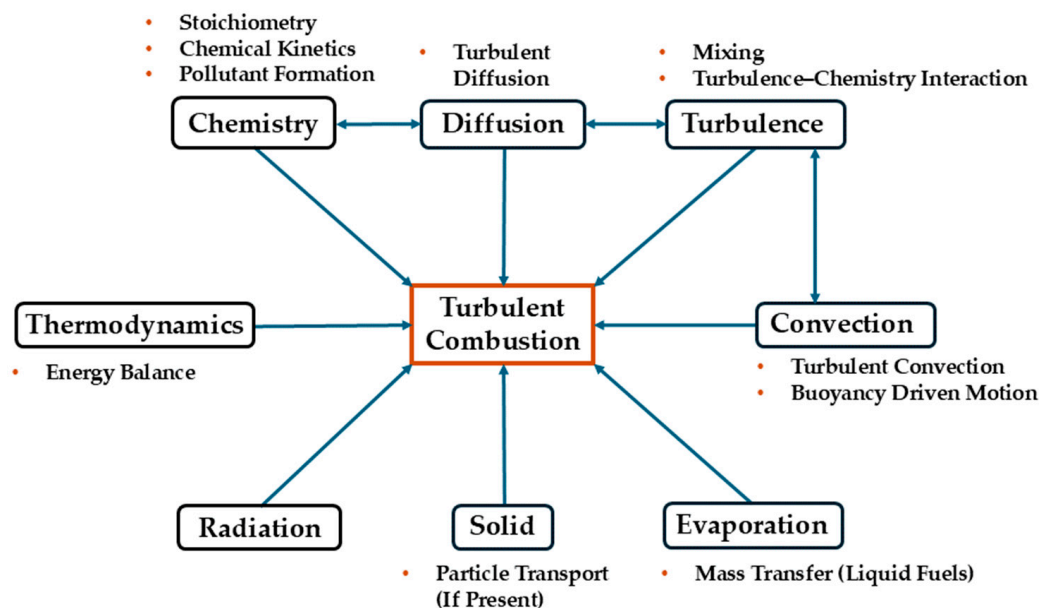


Figure 2. Multiphysics aspects of turbulent combustion.

Conventional approaches of simulating a turbulent reacting flow encounter several challenges that impact their accuracy and efficiency such as oversimplified assumptions, inadequate physical description, unreliable data, mesh dependence, high computational demand, etc. [16–19]. Machine learning (ML), however, offers the potential of revolutionizing the approach to understand and simulate this intricate phenomenon by overcoming the conventional limitations. It uses simulation or experiment data to analyze and find patterns for predicting results without any explicit physical model. This method offers a new standard in turbulence modeling by utilizing data-driven algorithms to improve predicted accuracy at lower computational costs and reduce the requirement for precise physical descriptions. Furthermore, the continuous advancement in Neural Networks has introduced new possibilities for addressing the complexities involved in modeling complex chemical kinetic mechanisms in combustion processes. This has led to significant improvements in both computational efficiency and accuracy under various conditions [20,21].

Turbulent reacting flow, with its widespread relevance across industries, presents a unique opportunity for machine learning applications. It enhances predictive skills, enabling more precise projections of flow patterns and assisting in the design and optimization of combustion systems with better efficiency and reduced emissions [22]. Additionally, this approach enables the development of simplified models and real-time control systems that can reduce processing demands while maintaining the essential characteristics of turbulent flows [22]. This integration not only simplifies operational processes but also strengthens environmental compliance and safety in industry applications.

ML application in turbulent combustion systems is the key focus of this study. In recent years, there has been an increasing interest in the application of machine learning and deep learning techniques to the study of ignition [23] and turbulent combustion [24]. ML can improve the modeling of turbulent flame propagation significantly by enhancing prediction skills and simplifying intricate simulations. Deep Neural Networks (DNNs) provide an efficient prediction of flame behavior in turbulent conditions by effectively capturing the key dynamics [25]. ML methods can assist creating sub-grid models for turbulent combustion simulations. These methods help to overcome the difficulties of combining fluid mechanics with chemical kinetics, resulting in enhanced accuracy and computational efficiency [26]. These advancements provide essential tools for optimizing combustion processes and building combustion systems that are safer and more efficient.

The ability of machine learning to learn directly from abundant data generated from simulations and experiments presents a viable alternative for modeling unresolved terms

in the complex transport equations governing turbulent reacting flows. The modeling of unresolved terms in the highly non-linear transport equations of turbulent and reacting flows is a complex and challenging task. However, the ability to “learn” directly from the data generated from the simulations and experimental studies offers a promising alternative [27]. Machine learning extracts useful information using the resolved database from conventional simulation and creates new models for predicting results for different input parameters.

This article aims to provide a comprehensive overview of the integration of machine learning techniques in simulating turbulent reacting flow along with its inherent challenges in applying these techniques and explore potential benefits, limitations, and future research prospects. Additionally, this study will present ML models for predicting plasma-assisted ignition kernel growth and a comparison of the predictions against Computational Fluid Dynamics (CFD)-simulated results, providing an extensive evaluation.

2. Challenges in Turbulent Combustion

The chaotic and irregular fluctuations in the flow field present numerous challenges for both the experimental studies and computational modeling of turbulent combustion. Because of the complex nature of turbulent combustion, a variety of problems [3] are associated with turbulent combustion, such as the following: (i) A thorough understanding of the fluid-mechanical properties of the combustion system is essential to precisely trace the transfer phenomena in turbulent flames, including heat transfer, molecular diffusion, convection, and turbulent transport [2,28]. (ii) Detailed chemical reaction schemes are necessary to accurately predict the fuel consumption rate, combustion products, and pollutant formation [29,30]. (iii) Detailed chemistry knowledge is vital to estimate reaction zone, ignition, stabilization, or extinction [29]. (iv) Multiphase (liquid and solid fuel) combustion processes can be encountered in turbulent combustion [31,32]. (v) Radiative heat transfer is produced within the turbulent flame and is carried by the flow motion [33–35].

The large and complex scales of turbulent combustion, from big flow structures to small chemical reactions, require new and advanced solutions beyond traditional methods.

3. Conventional Turbulent Combustion Modeling

Due to the challenges associated with turbulent combustion, modeling this specific type of combustion is a very broad subject. An estimated result of turbulent combustion phenomenon in a realistic combustion system in which all turbulence scales are fully resolved is exceedingly challenging with the available computational resources.

The turbulent combustion field has seen substantial advancements since the initial development of turbulent combustion modeling. In the past few decades, turbulence models based on the Reynolds-averaged Navier–Stokes (RANS) and Large-Eddy Simulation (LES) frameworks have been developed and applied in various engineering applications [36]. The advancement of turbulence models for non-reactive flows has inspired similar approaches [37] for turbulent reactive flows that subsequently led to the development of turbulent combustion models. However, the turbulence models require closure hypotheses that are used for approximating unknown turbulent quantities. These unknown variables are dependent on dimensional arguments and empirical data, which make turbulent combustion modeling difficult due to the inherent uncertainties and variability in different flow conditions, leading to potential inaccuracies [38].

The advent of CFD and the availability of more advanced combustion measurement techniques have facilitated further developments in the field. This progress can be attributed to several key factors. Firstly, the availability of advanced computational and experimental resources has allowed for more realistic simulations of combustion, with better descriptions of both flow dynamics and chemical reactions. It has also enabled the development of new approaches in turbulent combustion simulations, enabling direct computations of previously unresolved physical phenomena. Furthermore, the increasing

need for designing efficient and clean combustion technologies has also motivated the development of these advanced simulation techniques [39].

Nowadays, scientific computing provides an alternative method to collect multi-scale information, with CFD serving as a pivotal role in the design process [40]. Common challenges encountered in the numerical modeling of turbulent combustion include (i) complexity and diversity of spatio-temporal scales such as size and time scales [41], (ii) high degree of nonlinearities in flow dynamics and chemical reactions, and (iii) unpredictable nature and (iv) strong interaction among various subprocesses [24,42].

The critical need to address fluid engineering challenges has driven the development of turbulence models, which can be systematically derived from the Navier–Stokes equations to a certain extent. Although turbulence is a central and complex issue in classical physics, it remains only partially understood. The conversion of chemical energy to thermal energy through numerous chemical reactions within fluid turbulence makes turbulent combustion an extraordinarily complex problem, both in terms of fundamental understanding and predictive modeling.

4. Scopes of ML in Turbulent Combustion Models

Using the principal modeling strategies, turbulent combustion models can be categorized based on different parameters, such as the following:

Flamelet Model: The flamelet model of turbulent combustion characterizes the turbulent flame as a collection of laminar flame elements embedded within a turbulent flow. This approach, based on either the RANS or LES framework, is still being developed to address additional complexities, such as heat losses and spray dynamics. The integration of machine learning with Flamelet-Generated Manifold (FGM) models can help researchers automate the projection of one-dimensional flamelet solutions [43]. This approach makes it easier to accurately measure and understand the chemical properties in fluid dynamics simulations, enhance the prediction ability, and optimize combustion processes across different scenarios [43,44].

Conditional Moment Closure Model: Conditional Moment Closure (CMC) methods are relatively recent for turbulent reacting flows. Conceptually, it has been developed as a mixture fraction-based method for modeling non-premixed turbulent combustion with the fundamental concept of utilizing the strong correlation between reactive scalar species and the mixture fraction [45]. Machine learning can be used to enhance the estimation of conditional source terms, which is critical for accurate simulation. This strategy can use the extensive datasets from past experiments or simulations to analyze intricate patterns to increase the quality of predictions associated with reactive scalars and mixture fractions.

Probability Density Function Model: Probability Density Function (PDF) methods offer an effective solution to closure problems by incorporating the effects of turbulent fluctuations in both velocity and chemical composition within CFD models of turbulent reacting flows. Machine learning can benefit PDF models, particularly through the improved modeling of turbulent variations in velocity and chemical composition [46]. The integration of machine learning methods, such as Gaussian Mixture Models [47], facilitates a more detailed and accurate modeling of turbulent reactive flows and increases the credibility and precision of CFD models. This approach offers a more advanced approach for capturing the intricate dynamics within combustion systems.

Multiple Mapping Conditioning Model: Multiple Mapping Conditioning (MMC) is a recent addition to the turbulent combustion modeling approach [48]. It integrates the features of PDF, CMC, and mapping closure models. MMC serves as a framework for turbulent combustion modeling, containing a general set of principles and equations that can be adapted to develop specific MMC-based models tailored to particular turbulent combustion challenges [49]. Machine learning has the potential to significantly improve MMC models through enhancing the integration and modeling of the PDF, CMC, and mapping closure models [49]. By employing data-driven insights, machine learning can help

these elements to enhance the accuracy of predictions in turbulent combustion scenarios and, thus, improve the analytical abilities of MMC models.

Linear-Eddy Model: The Linear-Eddy Model (LEM) resolves the relevant advection–diffusion–reaction couplings in one spatial dimension by introducing a “triplet map”, which simulates the impact of an eddy turnover on property profiles along a hypothetical line of sight [50]. Using Artificial Neural Networks (ANNs), the LEM can effectively handle the complex coupling between turbulence and chemistry that takes place at smaller scales [51,52]. This approach offers a flexible adaptation of model parameters in response to new data, leading to accurate and efficient simulation.

One-Dimensional-Turbulence Model: The One-Dimensional Turbulence (ODT) model offers an innovative and efficient multiscale approach to integrate the processes of reaction, diffusion, and turbulent transport. ODT can be utilized independently for modeling simple turbulent flows, and it supports various formats for describing both spatially and temporally developing flows [53,54]. It can also be applied within a coupled multiscale framework using the ODT-LES approach [55]. Deep learning methods, such as Neural Networks, can facilitate the dynamic optimization of parameters in One-Dimensional Turbulence models and improve their potential to correctly approximate intricate interactions between turbulence and chemical processes within a simplified 1-D framework.

Unsteady Flame-Embedding Model: The Unsteady Flame-Embedding (UFE) model captures the transient flow–flame interactions, such as extinction, re-ignition, and historical effects, through embedded simulations at the sub-grid scale [56]. Similar to the flamelet approach, it considers the flame as a collection of locally one-dimensional flames [56]. A series of these elemental 1-D flames is used for directly representing the turbulent flame structure at the sub-grid scale [57]. Machine learning can improve Unsteady Flame-Embedding models by accurately and efficiently capturing complex sub-grid flame dynamics, such as extinction and re-ignition. This can optimize the representation of combustion processes within a reduced-order framework allowing the simulations to be much more precise and faster.

5. Machine Learning Integration in Turbulent Combustion

ML algorithms process large sets of data to find patterns and underlying mechanisms. By utilizing these insights, they can generate predictive models that are capable of addressing complex problems and making data-driven decisions. In this digital era, high-performance computing plays a crucial role in managing large volumes of data and accelerating the simulation of physical phenomena, data mining, and Artificial Intelligence (AI). The dominant performance of GPUs with their exceptional parallel computing capabilities further improves the speed of computation and simulation tasks. Training machine learning models on extensive datasets can, therefore, be efficiently executed on GPUs using deep learning frameworks like TensorFlow and PyTorch with minimal effort [58]. Given the rapid advancements in ML, its ease of deployment, and the improvements in hardware performance, machine learning has increasingly spread into combustion research area, offering solutions to many of the field’s most challenging problems.

Machine learning can be broadly categorized into three fundamental components: models, learning criteria, and optimization. ML models undergo training through an optimization process. Various optimization algorithms are employed, including gradient descent, stochastic gradient descent, adaptive moment estimation, and Newton’s method. A well-trained ML model should exhibit strong generalization capabilities [59]. Several approaches, such as dataset splitting, cross-validation, and early stopping, are used to improve a model’s generalization ability. Before training a machine learning model, the dataset is typically divided into two sets: a training set and a test set. The training dataset is used to train the model, while the test set is used to evaluate its generalization ability. Cross-validation involves using different subsets of the data to alternately train and test the model across multiple iterations. Early stopping is applied to achieve the minimum error on the test dataset before the model begins to overfit.

Recent advancements have established ML as a transformative tool in the study of turbulent combustion, addressing a wide range of physical phenomena, such as turbulence, chemical reactions, and heat transfer, which interact in complex and nonlinear ways. ML algorithms utilize the vast amounts of combustion data to analyze and identify patterns and correlations that are difficult to discern through traditional analysis methods. In the context of turbulent combustion, ML algorithms are applied to the following:

- Predict turbulent flame behaviors: ML algorithms can be trained on large sets of experimental or simulation data for predicting the behavior of turbulent flames under different conditions. This can give a better understanding of flames' reactions to pressure, temperature, and fuel composition changes [60].
- Optimize combustion processes: ML can be utilized to optimize combustion processes by predicting the optimal fuel–air ratio, the optimal temperature distribution, and other parameters that can affect combustion efficiency and emissions [61–63].
- Develop reduced-order models: ML can simplify turbulent combustion models, which can capture the essential physics of the problem while reducing computational cost [64–66].
- Identify and classify combustion regimes: ML algorithms can identify and classify different combustion regimes depending on the characteristics of the flame, such as flame structure, stability, and extinction [67,68].

Machine learning models can primarily be categorized into three types: supervised learning, unsupervised learning, and reinforcement learning, each involving various specific models [69].

Supervised Learning: Supervised learning (Figure 3) is one of the most widely used ML techniques in turbulent combustion. In this approach, a model is trained on a labeled dataset, where the input variables represent the features, and the output is the target or label [70,71]. The purpose of this method is to develop a function that can map inputs to outputs, enabling the model to make predictions on new, unseen data. Supervised learning can be applied to predict various areas of interest in turbulent combustion, such as flame speed, pollutant formation, or temperature profiles. Supervised learning algorithms commonly applied in turbulent combustion include Linear Regression, Support Vector Machines (SVMs), Decision Trees (DTs), and Neural Networks [65,70,71].

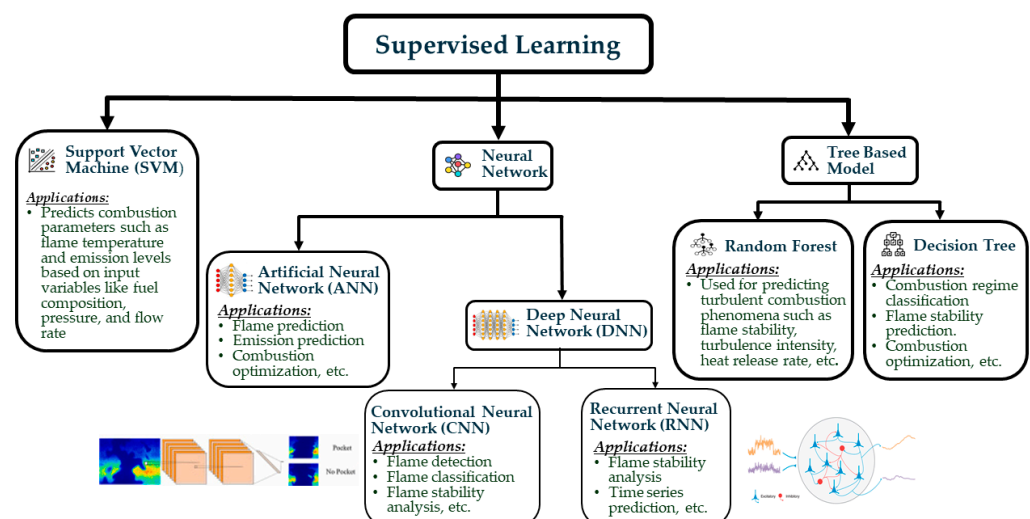


Figure 3. Classifications of supervised learning applications in turbulent combustion.

A typical application of supervised learning in turbulent combustion is to use Neural Networks, which are able to capture complex relationships between inputs and outputs. With the ability to approximate complex functions in a flexible manner [72], Neural Networks have emerged as the most popular supervised learning method in recent times [69].

Neural Networks can be either supervised or unsupervised, depending on the nature of the objective function, although they most commonly appear in supervised learning applications. In general, there are three key types of Neural Networks: Artificial Neural Networks (ANNs), Convolutional Neural Networks (CNNs), and Recurrent Neural Networks (RNNs). The ANN approach, along with its hybrid variations, shows great promise in handling the nonlinearities and complexities inherent in complex chemical processes [73], such as turbulent combustion. Deep Neural Networks (DNNs) consist of additional layers, neurons, and intricate architectures, enabling them to extract more features from raw input data. CNNs and RNNs are widely used deep learning models that demand larger datasets for training. CNN is mainly applied in the study of visual Neural Network representations [74] and has been applied to the combustion field, including areas such as unresolved flame surface wrinkling and temperature distribution modeling [75]. RNN is inherently well suited for handling time-series or sequential data and can be applied to predict the progression of flames over time [76], such as temperature or pressure measurements, and make predictions about future behavior.

Unsupervised Learning: Another ML technique used in turbulent combustion is unsupervised learning (Figure 4). Unlike supervised learning, the unsupervised learning model operates without any supervision. It involves training a model on an unlabeled dataset, with the goal of discovering patterns and relationships within the data [77,78]. Unsupervised learning can be used to analyze large sets of combustion data, such as temperature, pressure, and species concentrations, to identify patterns and relationships between variables. A common application of unsupervised learning in turbulent combustion includes the analysis of experimental or numerical simulations data to identify coherent structures, such as vortices or flames, that are responsible for mixing, heat transfer, and chemical reactions [52].

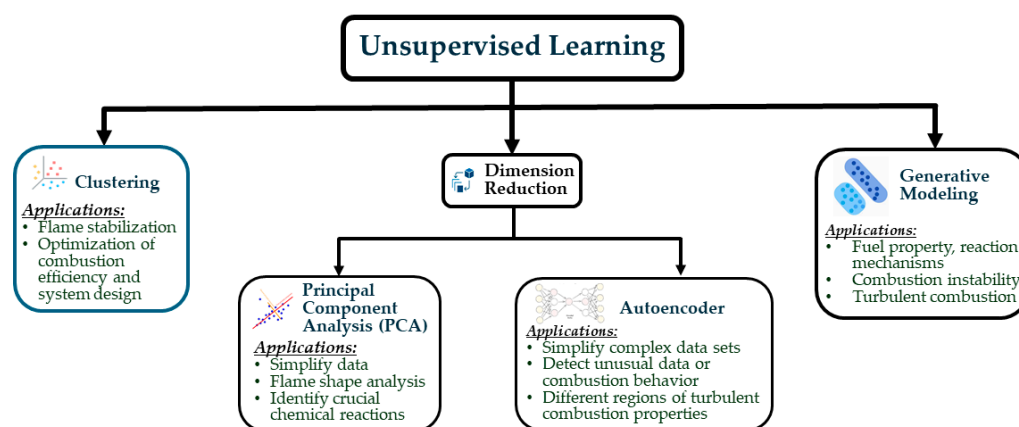


Figure 4. Classifications of unsupervised learning applications in turbulent combustion.

Unsupervised learning models are used for tasks like clustering data points based on similarity, detecting anomalies, identifying latent variables, reducing dimensionality, and generative modeling. Unsupervised learning algorithms used in turbulent combustion include clustering, principal component analysis, deep autoencoders, etc. The clustering process organizes a set of objects into multiple groups based on their similarities, without requiring labeled data, making it useful for pattern recognition and data compression. Popular clustering techniques include K-means clustering [79] and Self-Organizing Map (SOM) [80]. Clustering algorithms can group similar patterns and reveal the spatial and temporal organization of turbulent flows [81,82]. These algorithms are useful tools for grouping combustion data and thereby enhancing the training process of supervised learning models. Dimension reduction converts data from a high-dimensional space into a lower-dimensional space. Principal Component Analysis (PCA) is a widely used method for feature extraction and dimensionality reduction that identifies the most important variables in the dataset. An autoencoder is a type of Artificial Neural Network (ANN) used

for dimensionality reduction in an unsupervised approach, and it can also be applied for tasks such as anomaly detection and image denoising. Additionally, generative modeling is an unsupervised learning technique that can be trained to generate new examples that share the same statistical properties as the training data. In combustion research, generative modeling can convert low-resolution combustion images to high-resolution images.

Reinforcement Learning: Reinforcement Learning (RL) (Figure 5) is a machine learning approach where an agent is trained to make decisions by receiving feedback from its environment. It involves learning through trial-and-error exploration. Four key components in this process are the agent, environment, actions, and rewards [83,84]. Throughout the learning process, the agent learns to take actions within the environment that maximize the cumulative rewards. In turbulent combustion, RL is used for optimizing combustion processes in real time by training an agent to make decisions that maximize a specific objective like fuel efficiency or emissions reduction [64,85].

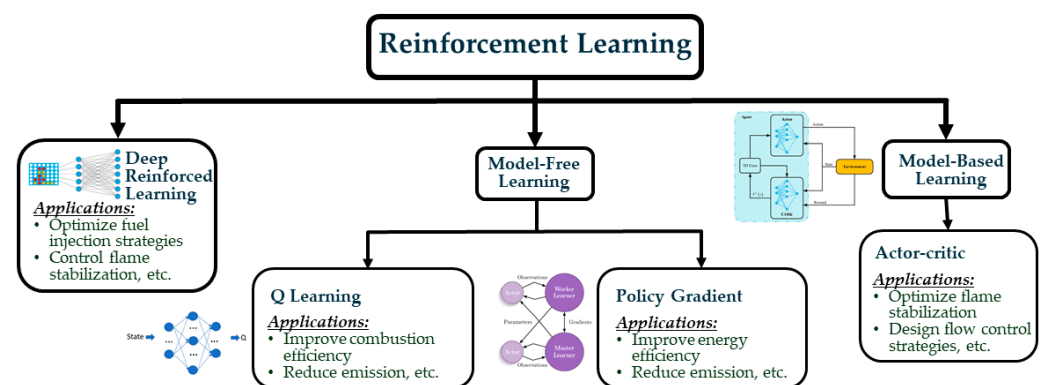


Figure 5. Classifications of Reinforcement Learning applications in turbulent combustion.

A core challenge in applying RL to turbulent combustion is managing the high-dimensional state space and action space, which makes it difficult to learn an optimal policy using traditional RL algorithms [86]. To address this challenge, researchers have developed a variety of advanced RL techniques. Reinforcement Learning algorithms can generally be categorized into two classes- model-based and model-free [87,88]. In model-free reinforcement learning, the agent learns through direct interaction with the actual environment, whereas in model-based reinforcement learning, the agent learns by engaging with a model of the real world. One approach to applying Reinforcement Learning to turbulent combustion involves modeling the combustion system as a Markov Decision Process (MDP). In this approach, the system's state is defined by the current values of relevant variables, such as temperature, pressure, and species concentrations [89]. The agent then takes actions that change the state of the system and receives rewards or penalties based on the resulting changes. Reinforcement Learning can also be used to optimize control policies for complex combustion systems, such as those with multiple inputs and outputs. In this case, the agent learns a mapping from the current state of the system to the optimal action, which can be used to develop closed-loop control systems that can adapt to changing operating conditions. Another type of Reinforcement Learning (RL) is known as Deep Reinforcement Learning. This type of RL employs Deep Neural Networks to estimate the value function or policy function. A comparison of these different algorithms in the context of turbulent combustion is briefly described in Table 1.

Table 1. Types of machine learning algorithm and their applications in turbulent combustion.

	Description	Applications in Turbulent Combustion	Comments
Supervised Learning	Model is trained using labeled data, meaning correct output is known for each input. The model then uses this training to predict results based on new, unseen data.	Supervised learning can be used to classify different types of turbulent combustion behavior, such as premixed vs. non-premixed flames. It can also be used to predict combustion emissions based on input parameters such as fuel type and temperature [90].	Pros: High accuracy, direct feedback mechanism, interpretable models, and wide real-world applicability. Cons: Dependency on labeled data, potential for overfitting, time-consuming labeling, and limited to training data patterns.
Unsupervised Learning	In the unsupervised learning process, the model is provided with unlabeled data, and it independently identifies patterns or relationships within that data.	Unsupervised learning is applied to identify clusters or patterns in data, collected from turbulent combustion processes, such as grouping the same kind of flame structures or identifying common forms of combustion instability. It can also produce high-resolution combustion images from low-resolution ones [64].	Pros: No label dependency, data structure discovery, feature extraction capability, and anomaly detection suitability. Cons: Indeterminate outcomes, potential prediction inaccuracy, algorithmic complexity, and subjective evaluation challenges.
Reinforcement Learning	Reinforcement Learning is a process where learning occurs through trial and error, with feedback provided in the form of rewards or penalties for specific actions. Over time and with adjustments, Reinforcement Learning models learn to make decisions that maximize rewards.	Reinforcement Learning optimizes the operation of a turbulent combustion system, such as by controlling the air/fuel ratio or adjusting the combustion chamber geometry to minimize emissions or maximize efficiency. It could also be used to develop control strategies for mitigating the turbulent combustion instability [86].	Pros: Optimized for decision-making, environment adaptability, exploration-exploitation balance, and real-time feedback incorporation. Cons: Extended training periods, reward function intricacies, and training instability.

6. Machine Learning Applications in Turbulent Combustion Modeling

Researchers have developed machine learning techniques with an aim to improve turbulence modeling particularly emphasizing predicting the nonlinear interactions between turbulence and combustion. Some approaches for modeling turbulent combustion, such as the steady flamelet and FGM methods, rely on precomputed simulations of laminar flames (Figure 6). In contrast, other techniques require the real-time calculation of the chemical source term at each grid node and time step [91]. These methods are Direct Numerical Simulation (DNS), PDF, unsteady flamelet, CMC, MMC, LEM, Thickened Flame Model, Partially Stirred Reactor (PaSR) method, etc. [92–94]. Flames are mostly turbulent in practical combustion chambers. The burning velocity of flames increases with the rise in turbulence intensity [95]. Without the use of any additional combustion model, using DNS for turbulent combustion simulation coupled with a detailed chemical mechanism is nearly impossible because of the unstable nature of turbulent combustion, the enormous demand for computational resources, the absence of comprehensive chemical mechanisms, and the limited applicability of the models [64]. Possible lower-resolution simulations require closure models. However, current state-of-the-art closure models often fail to accurately capture key dynamics in certain turbulent combustion regimes, leading to potential inaccuracies in predictions [96].

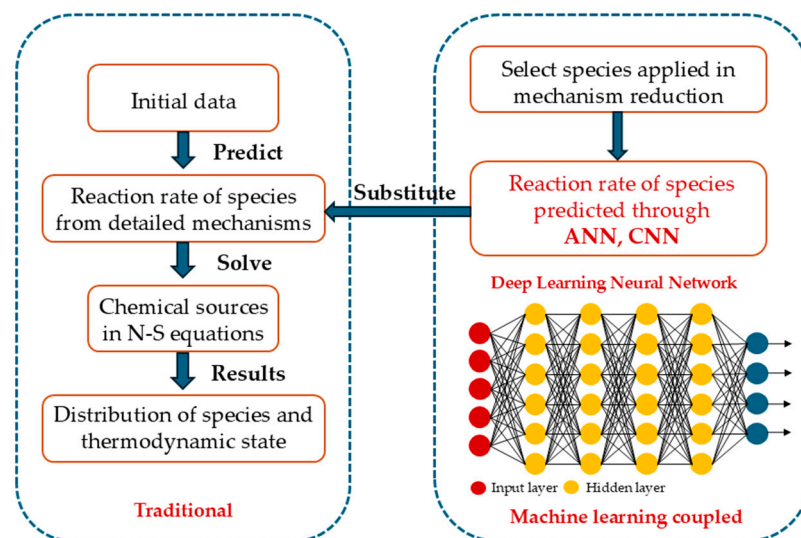


Figure 6. Machine learning integration with traditional CFD models. Reprinted with permission from [64]. Copyrights 2022 Elsevier.

The use of machine learning methods for chemical reaction calculations offers two major advantages: increased calculation speed and reduced memory usage [97]. Since a machine learning model primarily stores its structural information and activations, it typically requires minimal storage space. Furthermore, ML methods offer greater accuracy compared to traditional tabulation techniques [64]. Machine learning algorithms, such as Naive Bayes, SVMs, logistic regression, and others, can suggest adjustments to the operating parameters of a scientific model for a complex system, based on related post-operational data [98]. The established methods for the simulation of turbulent combustion typically involve one or more of the following three strategies: (1) chemistry representation; (2) sub-grid scale modeling; (3) surrogate/specialized solver [22].

Direct Numerical Simulation (DNS) databases, combined with machine learning techniques, particularly Neural Networks, serve as effective tools for extracting valuable information and identifying patterns within these databases for modeling purposes [99]. Lapeyre et al. [75] applied the results of the DNS simulation of a premixed turbulent flame to train a CNN model to approximate the sub-grid flame surface density. Similarly, Barwey et al. [15] used a CNN model to predict the three velocity components within premixed flames in a swirl combustor based on a series of time-resolved Planar Laser-Induced Fluorescence (PLIF) images of hydroxyl radicals (OH). The flamelet and PDF-like models generate data in real time and can be utilized to calculate unconditional means for reactive scalars and their associated chemical source terms [100]. An et al. [101] employed ANN to accelerate the computations of hydrogen/hydrocarbon combustion chemistry in a supersonic engine environment, achieving computation speed-ups ranging from 8 to 20 times compared to a conventional Ordinary Differential Equation (ODE) solver. Mal'sagov et al. [21] presented a five-layer Neural Network to simulate hydrogen combustion at varying pressures, achieving two to three times faster computation time than traditional methods while maintaining high accuracy and a mean standard error. Weymouth et al. [102] introduced a model that uses deep learning, based on the spanwise-averaged Navier–Stokes equations. This approach aims to decrease the computational costs associated with the inherently three-dimensional nature of turbulence by applying dimensionality reduction. In the case studied, the model achieved 90–92% correlation to the original 3-D system while using only 0.5% of the CPU time.

6.1. ML Application Using Image Processing

One of the approaches of using machine learning in turbulent combustion is to analyze flame images (Figure 7) [103]. Lee et al. [104] applied transfer learning to train a CNN model

for classifying impinging jet flames into four distinct regimes characterized by unique thermoacoustic oscillations. The CNN model achieved 93.6% accuracy in this classification task. Some limitations of their study came from the Particle Image Velocimetry (PIV) flow field patterns and the necessity of testing each regime at least once. Shamsudheen et al. [105] used K-Nearest Neighbors (KNN) and SVM models to classify combustion events in a Homogeneous Charge Compression Ignition (HCCI) engine. The study found that the SVM method outperformed KNN, achieving higher accuracy and better generalization, with a 93.5% accuracy compared to KNN's 89.2%.

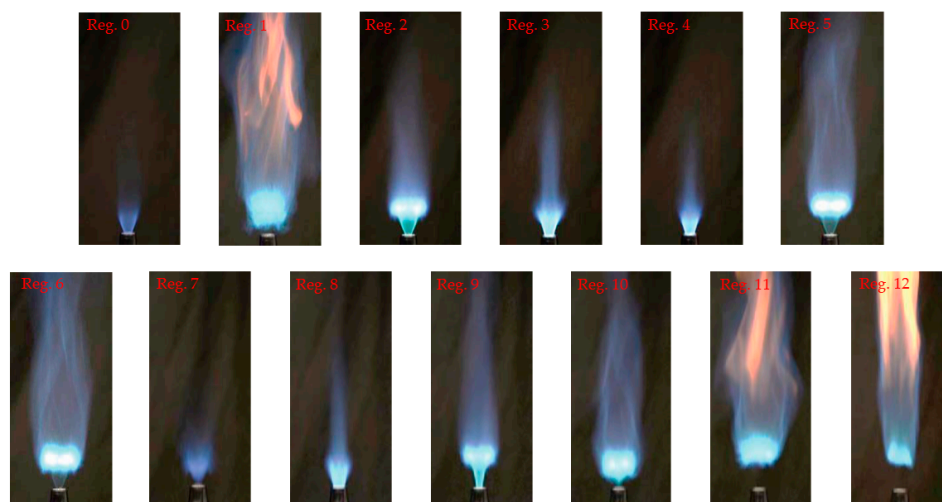


Figure 7. Examples of the flame images representing the captured combustion regimes. Reprinted with permission from [106]. Copyrights 2018 AIP Publishing.

Gobyzov et al. [106] discussed the use of CNN to classify combustion regimes (Figure 7) based on flame imaging. The CNN achieved an average accuracy of 97.9% in classifying the flame images into various combustion regimes. The model was particularly effective, with most combustion regimes classified with an accuracy close to 99%. However, certain regimes (specifically regimes 0, 3, 4, 7, and 8 in Figure 7) showed slightly less accuracies ranging from 95% to 97%, mainly due to the visual similarity of these flame images. Comparison with other datasets was performed to validate the overall performance of the CNN model. It was also trained and tested on standard datasets like Modified National Institute of Standards and Technology (MNIST) and Canadian Institute for Advanced Research-10 (CIFAR-10), achieving accuracies of 99.4% and 85.6%, respectively.

6.2. ML Application in Chemical Composition

Combustion chemistry is crucial in designing an efficient and low-emission combustion system. Although supercomputing methodologies are continuously progressing, the degrees of freedom necessary to fully describe detailed combustion chemistry cannot be fully implemented in numerical simulations of large-scale combustion systems. To address this problem, various methods have been proposed to simplify and optimize extensive chemical kinetic schemes. These methods include Quasi-Steady State Approximation (QSSA), partial equilibrium, Directed Relation Graph (DRG), Directed Relation Graph with error propagation, DRG-Aided Sensitivity Analysis (DRGASA), and the elimination of unimportant reactions [107]. One of the primary challenges in combustion modeling with detailed chemistry mechanisms in CFD methods is the enormous computational demand resulting from the need to solve numerous nonlinear stiff chemical kinetics equations. Even after reducing the number of differential equations to be solved, the stiff nature of these differential systems associated with combustion chemistry requires substantial CPU time for their integration, limiting the ability to perform numerous simulations needed for optimizing the combustion system design [108]. On top of that, the complex chemi-

cal properties of different fuels lead to a significant increase in the number of reactants and equations, making the integration of detailed mechanisms in combustion simulations exceedingly difficult. The problem with integrating chemistry can be mitigated by using tabulation, where the reaction source terms are retrieved from a database of precomputed chemical integrations. The Look-Up Table (LUT) [109] tabulation method retrieves data by interpolating from a table of precomputed values. However, the memory requirements for this process increase exponentially with the number of species, making it suitable only for small mechanisms. A more advanced technique involves combining Intrinsic Low-Dimensional Manifolds (ILDMS) [110] with In-Situ Adaptive Tabulation (ISAT) [111], where the table is generated during the simulation. While this approach can reduce CPU time, it still demands significant memory resources.

These computational limitations have led to the adoption of machine learning approaches, specifically ANN, to address chemistry reduction, time integration, and the development of data-driven models for turbulent combustion. ANN can be applied to various tasks, including nonlinear regression. For a given chemical mechanism, species concentrations after a reaction time step depend on the initial condition, and ANNs can be trained to estimate these functions. Christo et al. [112] used ANN for combustion chemistry tabulation by introducing ANN to represent a simplified three-step mechanism for $H_2/CO_2/O_2$ mixtures, which was further applied in PDF simulations of turbulent flames [113,114]. The simulation results demonstrated strong alignment with the Direct Integration (DI)-simulated results. As the number of species increases, the composition space expands exponentially, making it challenging to tabulate the entire space with a single ANN. To address this issue, Blasco et al. [115] proposed a partitioning method that splits the composition space into multiple subdomains based on mixture fraction or temperature, with each subdomain being modeled by a separate ANN. This approach was applied to simulations of Plug-Flow Reactors (PFRs) and Partially Stirred Reactors (PaSRs), showing reasonable results. In their study, they focused on implementing a Neural Network to predict chemical reactions in H_2/CO_2 turbulent jet diffusion flames. The Neural Network approach was compared with traditional methods like DI and LUT, highlighting improvements in computational performance and accuracy. They also introduced a Self-Organizing Map (SOM) to cluster the composition space into multiple subdomains [116]. Direct Integration (DI) requires the longest CPU time but offers lower accuracy. The Look-Up Table method provides moderate CPU efficiency with improved accuracy. Neural Networks, on the other hand, significantly reduce CPU time while delivering the highest accuracy among these methods. (Table 2)

Table 2. Comparison of CPU Time and RAM requirements across various methods for managing chemistry. Reused with permission from [113]. Copyrights 1996 Elsevier.

Jet Velocity (m/s)	Method	RAM (Megabytes)	CPU Time (min)	CPU Ratio
50	Look-Up Table	13.31	107	2.9
	Neural Model	10.02	119	3.2
80	Look-Up Table	13.31	176	1.9
	Neural Model	10.02	170	1.8
130	Look-Up Table	13.31	242	--
	Neural Model	10.02	204	--

Here's a table illustrating the comparison of computational efficiency and accuracy among different methods used for simulating turbulent combustion chemistry:

Ideally, ANNs should possess strong generalization capabilities, enabling their application to a wide range of real-world problems. However, in the studies mentioned earlier, the same problem was used for generating the training dataset and to test the ANNs. As a result, the problem must be simulated in advance using DI whenever ANNs are applied to a new problem. However, that diminishes the speed advantage. To ensure ANNs have

robust generalization ability, the training data must cover the appropriate composition space that aligns with realistic simulations. Chatzopoulos et al. [117] presented an approach of generating training data using an established problem that involved dynamic flamelet simulations and a Rate-Controlled Constrained Equilibrium (RCCE)-reduced chemistry mechanism. The training data were segmented into 400 subdomains using a SOM, with each subdomain being fitted by an individual Multilayer Perceptron (MLP). This SOM-MLP approach was further developed by Franke et al. [118] who incorporated extinction events and combined it with the LES-PDF. The resulting LES-PDF-ANN methodology was then applied to simulate the Sydney turbulent flame, which featured significant levels of local extinction and re-ignition. The model showed a good agreement between the ANN and DI. An et al. [101] also applied the SOM-MLP methodology to simulate the hydrogen/carbon monoxide/kerosene mixture in a rocket-based combustor. The training data were generated through a RANS simulation, after which the ANNs were applied in an LES simulation, demonstrating strong agreement with the results from DI. Nikitin et al. [20] used ANN architecture to model the chemical kinetics of hydrogen combustion, which could predict the behavior of the chemical system over multiple time steps. The study reported a significant threefold acceleration in computation time compared to traditional numerical methods.

6.3. ML Application in Flamelet-Based Models

A flamelet is characterized as a thin, reactive-diffusive layer seamlessly integrated within a predominantly non-reacting turbulent flow field. In flamelet-based modeling, the turbulent diffusion flame is considered as a collection of stretched laminar flamelets [24]. Flamelet models offer a promising way of circumventing the computation of intensive transport of chemical species in CFD simulations of turbulent combustion. The concept is based on decoupling the chemistry from the physical space and solving them on a reduced mixture fraction space where only the important scalars are solved to determine the statistical moments of mass fractions and temperature. Instead of transporting all species and chemistry to each cell, these methods retrieve chemistry from the multidimensional manifold. These techniques can potentially minimize the computational costs by an order of magnitude [119].

Terrapon et al. [120] were one of the earliest to implement the flamelet model for supersonic combustion using a 3-dimensional manifold based on the steady flamelet equations. Berglund et al. [121] conducted a comparison between 1-D and 2-D manifold predictions for the LES of supersonic hydrogen combustion within a scramjet engine model. Overmann et al. [122] created a 3D-manifold-based flamelet model. In all these methods, compressibility effects were considered by tabulating the species' mass fractions and using a transport equation for total enthalpy. The species mass fractions were determined using the flamelet manifold, and the temperature was derived from the species mass fractions and enthalpy. Many scramjet simulations have been conducted using this similar Flamelet Progress Variable (FPV) approach [123,124]. However, these methods do not account for all the compressibility effects. The change in chemistry with respect to pressure is not captured accurately by these manifolds as the flamelet manifolds are generated for a constant pressure. Some of the studies used scaling relations to account for the differences in pressures. Quinlan et al. [125–127] carried out detailed studies with the FPV approach and demonstrated the importance and implementation of the pressure as an additional dimension. Ladeinde et al. [128,129] analyzed the impact of constant pressure manifolds and scaling relations to demonstrate the importance of pressure dependent manifolds for supersonic combustion. Also, many of these methods do not account for the unsteady flamelet formulation that plays a crucial role in auto-ignition events.

The study of turbulent flame evolution has gained significant attention, particularly in areas such as flame ignition, flame propagation, quenching, and pollutant formation, etc. [25]. The accurate prediction of turbulent flame evolution is, therefore, highly desirable. Direct Numerical Simulation (DNS) resolves both turbulence and flame scales in turbulent

flames, and many such studies have been conducted using DNS. For instance, Aspden et al. [130] have conducted a study on the turbulence effects on lean premixed hydrogen focusing on the roles of molecular and turbulent mixing processes. Gruber et al. [131] investigated flashback phenomena in premixed hydrogen/air flames at the boundary layer of a fully developed turbulent channel flow. Wang et al. [132–134] performed a series of DNS studies on experimental premixed jet flames, analyzing the structure and stabilization of flames, and turbulence–flame interactions. However, such DNS studies require substantial computational resources that highlight the need for more efficient methods to reduce the cost of predicting turbulent flame evolution.

For the CFD simulation, species' mass fractions are gained from the table as functions of the reaction coordinate via interpolation. While this leads to significant savings in runtime compared to a detailed chemistry approach, flamelet tables suffer from the problem of dimensionality as the table size increases. Hence, the memory requirements grow exponentially with the increase in input dimensions. The computational cost and complexity of interpolation also increase rapidly with additional input variables. So, rendering tabulated flamelet models are only feasible for low-dimensional tables.

One of the promising ways to solve these issues is the use of machine learning models to learn the flamelet tables where these models are trained to take the control variables as inputs and output the dependent variables. The primary advantage of this approach is the memory efficiency and incorporation of larger flamelet tables in CFD simulations of turbulent combustion. Machine learning models, such as ANN and CNN, can find complex and hidden patterns in data. By forming the highly nonlinear relationships, these models are applied in regressions and classifications. Therefore, machine learning can accurately and efficiently capture the dynamic flame characteristics of combustion systems.

According to the flamelet assumption, the turbulence reaction rate depends on the flame surface area. Therefore, it is crucial to evaluate the flame surface area in the sub-grid scale of LES. For the estimation of sub-grid-scale contribution, Lapeyre et al. [75] developed a CNN network designed to approximate sub-grid-scale flame surface density using the topological information of the progress variable. The training data were sourced from the DNS database of a methane–air slot burner. The input data for the CNN model consisted of the 3D-filtered progress variable derived from DNS data, while the output was the 3D-normalized flame surface density. By training the CNN model inspired by the U-net architecture [135], the model achieved high accuracy in predicting the flame surface density.

Ren et al. [25] studied predictive models for turbulent flame evolution using Long Short-Term Memory (LSTM) and CNN-LSTM in which they focused on two configurations: freely propagating turbulent premixed combustion and turbulent boundary layer premixed combustion. The models were validated against DNS data to evaluate their performance, and it was found that the CNN-LSTM model outperformed the LSTM model, as the CNN-LSTM model captures both spatial and temporal features of the flames, whereas the LSTM model only captures temporal features. The models' errors were mainly concentrated in regions with large scalar gradients.

Figure 8 describes the comparative analysis of the LSTM and CNN-LSTM models used to predict the evolution of methane (CH_4) mass fraction in freely propagating flames. The flame dynamics was characterized by the changing formations known as “peninsulas” of reactants and “pockets” of products. As time progressed, the size of the product pockets increased while the peninsula of reactants decreased. The LSTM model effectively captured the evolution of the pocket structures but encountered difficulties with the peninsula structures. In contrast, the CNN-LSTM model excelled in accurately predicting the evolution of both pocket and peninsula structures. Relative error metrics, defined as the difference between predicted and actual DNS values normalized by the maximum DNS value, were used to assess the model performance. The CNN-LSTM model exhibited smaller relative errors compared to the LSTM model, particularly near the thin flame front where both models tend to overestimate the CH_4 mass fraction. Overall, the CNN-LSTM model showed

better performance than the LSTM model in terms of predicting the complex dynamics of freely propagating flames.

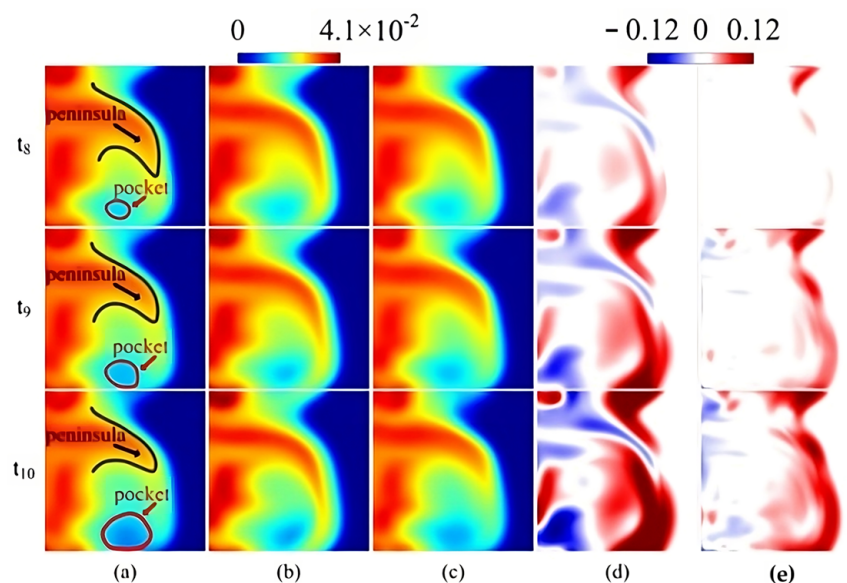


Figure 8. CH₄ mass fraction distributions in freely propagating flames: (a) DNS results, (b) LSTM predictions, (c) CNN-LSTM predictions, (d) LSTM prediction errors, and (e) CNN-LSTM prediction errors. The red line represents the product pocket, and the black line marks the reactant peninsula. Reprinted with permission from [25]. Copyrights 2021 Physics of Fluids.

Figure 9 shows the prediction of the CH₄ reaction rate in freely propagating flames, compared to DNS results and the distribution of relative errors. Figures 8b,c and 9b,c demonstrate the flame structure predicted by the models that closely matched with the DNS results, suggesting models' ability to accurately capture the overall flame structure. Figures 8d,e and 9d,e present the distributions of relative errors for both models, showing similar error patterns. The relative errors for the CH₄ reaction rate are notably larger than those for the CH₄ mass fraction likely due to the nonlinear nature of the reaction rates and species mass fractions. The models tend to overestimate the CH₄ reaction rate on the product side of the flame while underestimating it on the reactant side. These discrepancies suggest that, although the models are generally effective in replicating the flame structure, they struggle in accurately predicting the precise distribution of the flame reaction zone.

Owoyele et al. [136] introduced the Mixture of Experts (MoE) approach, a divide-and-conquer machine learning technique designed to learn flamelet tables. This method has been demonstrated and validated within the context of the Unsteady Flamelet Progress Variable (UFPV) model applied to Large-Eddy Simulations (LESs) of Engine Combustion Network (ECN) Spray A. The approach involves a system of Neural Networks consisting of a gating network classifier and multiple regression expert models. The gating network splits the flamelet table, while the regression models specialize in making predictions within specific regions of the manifold. The proposed model was then further validated using UFPV model used in the Reynolds-Averaged Navier–Stokes (RANS) simulation of Engine Combustion Network (ECN) Spray A [137]. Both of the validation showed that MoE was able to capture both global and local flame characteristics while enabling significant memory savings.

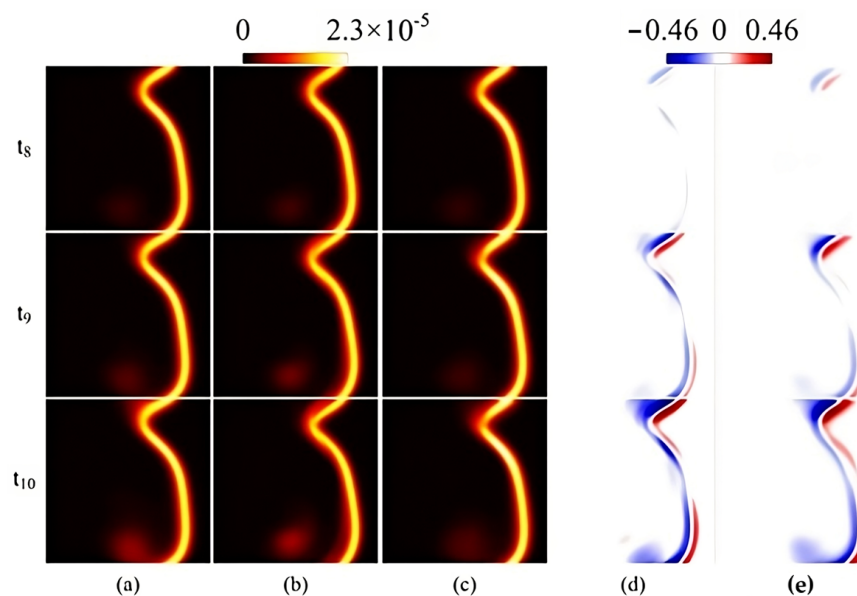


Figure 9. CH₄ reaction rate distribution in freely propagating flames: (a) DNS results, (b) LSTM predictions, (c) CNN-LSTM predictions, (d) LSTM prediction errors, (e) CNN-LSTM prediction errors. The unit of the reaction rate is mol·m⁻³s⁻¹. Reprinted with permission from [25]. Copyrights 2021 Physics of Fluids.

Kempf et al. [138] used ANN models to demonstrate steady laminar flamelet solutions and applied them to the LES of Sandia flame D. These models were later optimized by Ihme et al. [139] and used in the LES of a bluff-body swirl-stabilized flame. Hansinger et al. [140] trained an ANN model using FPV tables, which showed good agreement with conventional tabulated FPV simulations. The FPV models, however, do not have the extremely high CPU time demands for chemistry integration as seen in models where the chemistry is computed in real time, which made the need for tabulation less critical for these methods. [91]. Emami et al. [141] simulated a jet diffusion flame (CH₄/H₂ mixture) using a flamelet approach, incorporating ANNs in place of direct chemistry integration. The input variables in this approach included scalar dissipation, mixture fraction, and variance. This approach aligns with methods previously proposed by Kempf et al. [138] and Ihme et al. [139]. Demir et al. [119] presented the application of Deep Artificial Neural Networks to replace higher dimensional manifolds focusing on the integration of the UFPV model into the Viscous Upwind Algorithm for Complex Flow Analysis (VULCAN)-CFD code. To test and validate the implementation of transport equations and the interpolation of a multidimensional scheme, a supersonic hydrogen-air mixing layer was modeled. The UFPV-ANN approach was then validated in a 1-D context and a supersonic mixing layer simulation. Using the unsteady formulation, a multidimensional flamelet table was created, and a Deep Artificial Neural Network was trained using this manifold. The results suggested that the ANN approach could achieve the same outcomes as the memory-intensive Look-Up Table method.

7. New Insights into ML for the Prediction of Plasma-Assisted Ignition Kernel Growth

This section presents the results of machine learning methods, specifically Decision Trees (DTs) and Random Forests (RFs), for the spatio-temporal prediction of plasma-assisted ignition kernels in a stoichiometric methane/air mixture based on the initial degree of ionization. The training and testing were conducted using a 2-D DNS model for the ignition of a stoichiometric methane–air mixture. The concept of ignition kernel growth, which is the initial phase of the combustion process where a fuel–air mixture begins to react chemically under an external energy source, forming a stable flame, was applied. This stage is crucial as it dictates the characteristics of the resulting flame and,

consequently, the overall efficiency of the combustion process. Various factors, such as fuel type, mixture composition, and ignition source properties, influence ignition kernel growth. The introduction highlights the importance of understanding these factors to enhance combustion efficiency and reduce pollutant emissions. Plasma-assisted systems, which include nanosecond pulse and laser discharge techniques, can produce higher concentrations of reactive radicals, reduce the minimum ignition energy required, and ignite leaner mixtures. These capabilities make plasma-assisted ignition a promising technology for improving fuel economy and reducing Nitrogen Oxide (NO_x) emissions. However, traditional computational models used to study ignition kernel growth, such as CFD integrated with chemical kinetics, are limited by their reliance on extensive experimental data for validation. To address these limitations, this chapter proposes the integration of machine learning techniques into ignition kernel modeling. ML models, including Decision Tree (DT) and Random Forest (RF), offer new methodologies for predicting complex combustion dynamics without heavily relying on large datasets. These models can learn from limited data and generalize to new conditions, providing a powerful tool for predicting ignition behavior under varied operational scenarios. To evaluate the effectiveness of different ML models in predicting the growth and behavior of ignition kernels, comparing their performance using various statistical measures to determine their reliability and accuracy (Table 3). Several studies highlight the effectiveness of machine learning (ML) in ignition modeling [142]. This chapter presents a two-dimensional Direct Numerical Simulation (DNS) to analyze plasma-assisted ignition kernel growth, which was trained using an ML model. Machine learning models such as Decision Trees (DTs) and Random Forests (RFs) have been used to predict the behavior of key variables, such as temperature and the concentrations of CH and OH species, at different energy deposition levels.

Table 3. Comparison of Decision Tree and Random Forest model performance matrices for plasma-assisted ignition exploring T, OH, and CH features.

	T(K)		CH		OH	
	DT	RF	DT	RF	DT	RF
Mean Squared Error (MSE)	7.06×10^2	8.24×10^2	2.53×10^{-12}	2.68×10^{-12}	5.25×10^{-9}	6.44×10^{-9}
Mean Absolute Error (MAE)	4.04	4.46	1.20×10^{-7}	1.32×10^{-7}	7.14×10^{-6}	8.26×10^{-6}
Root Mean Sq. Error (RMSE)	26.6	28.7	1.59×10^{-6}	1.64×10^{-6}	7.25×10^{-5}	8.02×10^{-5}
Normalized RMSE (NRMSE)	0.0436	0.0471	4.57	4.71	0.333	0.369
Normalized MAE (NMAE)	6.64×10^{-3}	7.32×10^{-3}	3.44×10^{-1}	3.79×10^{-1}	3.28×10^{-2}	3.80×10^{-2}
Minimum Absolute Error	0	0	1.71×10^{-17}	9.81×10^{-13}	0	2.33×10^{-13}
Maximum Absolute Error	1.32×10^3	1.57×10^3	8.10×10^{-5}	8.16×10^{-5}	2.79×10^{-3}	2.91×10^{-3}
Correlation Coefficient	0.999	0.998	0.929	0.922	0.998	0.997
R ² (Coeff. of Determination)	0.997	0.997	0.859	0.850	0.996	0.995

The study uses detailed numerical simulations to model the dual-pulse laser-assisted ignition kernel growth, developed using a custom-made OpenFOAM solver in C++ and described in detail in Refs. [143,144]. A further testing of the model was conducted based on stochastic error evaluation, as detailed by Smirnov et al. [145]. The total error was determined by summing the relative errors in each direction, and, assuming a maximum allowable error for the simulation, the maximum allowable number of time steps was evaluated as described in [145]. The training datasets were obtained from the simulations under different ionization conditions, using a modified Latin Hypercube Sampling (LHS) technique to ensure a broad range of conditions for model training. The grid index term was defined for ML training, as shown in Figure 10, and corresponds to a specific point in the domain where ignition kernel parameters, such as temperature, were labeled to track and train data for various machine learning algorithms. The machine learning algorithms were trained at energy deposition levels of $n_{e,I}(0)$, $n_{e,II}(0)$, and $n_{e,III}(0)$ at time intervals of 30, 40, and 50 microseconds. The initial conditions for electrons and positive ions

are given by the following form, $n_e = n_e(0) \exp\left(-\frac{x^2}{x_{ch}^2} - \frac{y^2}{y_{ch}^2}\right)$, where $n_e(0)$ are the initial concentrations of electrons on the axis of the plasma channel, $x_{ch} = 100 \mu\text{m}$ and $y_{ch} = 500 \mu\text{m}$ are the sizes of the initial ionization region created by the UV pulse. The goal was to accurately predict performance metrics and spatio-temporal ignition kernels at a target, $n_{e,t}(0)$, energy deposition [$n_{e,I}(0) = 0.85 n_{e,t}(0)$, $n_{e,II}(0) = 1.15 n_{e,t}(0)$, and $n_{e,III}(0) = 0.9 n_{e,t}(0)$] (Figure 11). The electron temperature was initially set to 1 eV. The initial vibrational and gas temperatures were both set to 500 K. The mathematical model and energy deposition are described in [143–145].

Figure 11 illustrates a workflow for training and testing models to analyze plasma properties using two machine learning methods: Decision Tree and Random Forest. The training phase involves data from initial ionization levels $n_{e,I}(0)$, $n_{e,II}(0)$, and $n_{e,III}(0)$ with features such as temperature (T), Hydroxyl Radical (OH), and Hydrocarbon (CH) at three different time points: 30 μs , 40 μs , and 50 μs . The testing phase uses new initial ionization data $n_{e,t}(0)$ and the same features at the corresponding times to validate the models with the DNS model. The DNS results of Laminar Flame Speed and Damkohler number at the targeted initial ionization data, $n_{e,t}(0)$ are presented in Figures 12 and 13. Figure 12 shows the contour plots of the laminar flame speed (S_L) of the ignition kernel growth at 30, 40, and 50 microseconds in the baseline simulation. The laminar flame speed was calculated based on the flame progress variable and thermal diffusivity. The flame speed varies between 0 and 10 m/s, as indicated by the color bar. These contour plots demonstrate the growth and evolution of the ignition kernel, with clear increases in flame speed and structural complexity as the ignition kernel as time progresses.

The Damköhler number (Da), representing the ratio of the flow time scale to the reaction time scale, is a key indicator of the balance between chemical reactions and flow dynamics in ignition kernel growth. In regions with a high Damköhler number (≥ 50), seen as red in the figures, chemical reactions occur much faster than the surrounding flow, indicating rapid kernel growth and intense combustion. This is especially prominent at the interface of the ignition kernel, where the temperature and reactant concentrations are optimal for fast reactions. Over time (from 30 μs to 50 μs), the region of high Da expands along the kernel boundary, indicating that chemical reactions dominate at the growing interface. In contrast, lower Da regions both inside the kernel and in the surrounding area suggest that flow or mixing dominates over reactions, leading to slower combustion in those regions.

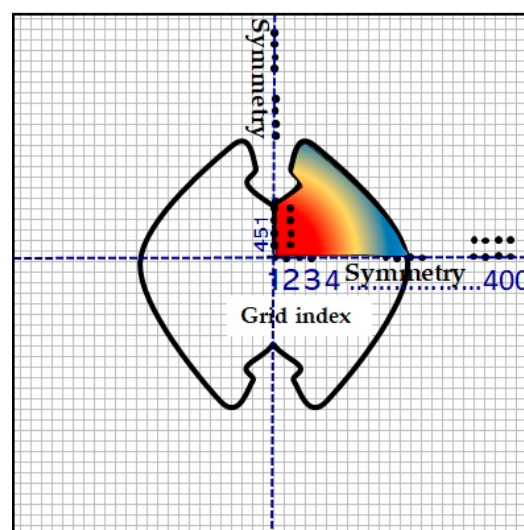


Figure 10. Grid index definition for ML model training and validation.

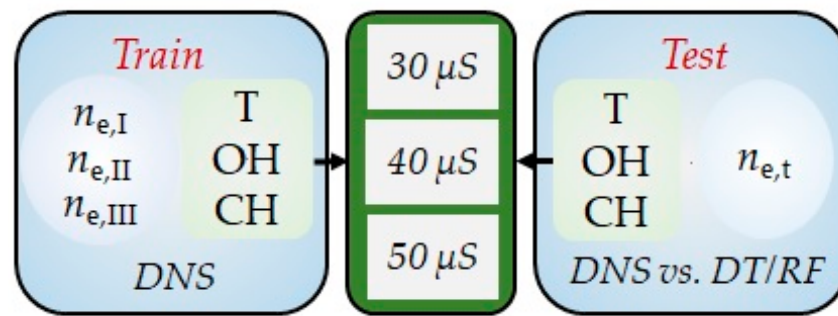


Figure 11. Model training and testing outflow for the ignition kernel prediction model.

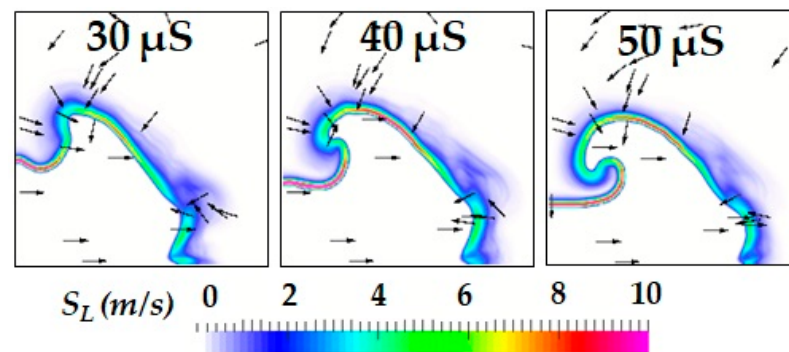


Figure 12. Evolution of laminar flame speed during ignition kernel growth at 30, 40, and 50 microseconds and velocity vectors (arrow) from DNS simulation (Visualization area: 2 mm × 2 mm).

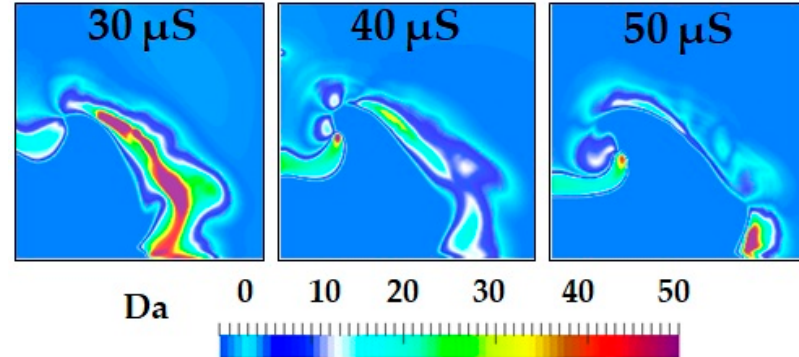


Figure 13. Evolution of Damköhler number (Da) during ignition kernel growth at 30, 40, and 50 microseconds and velocity vectors (arrow) from DNS simulation (Visualization area: 2 mm × 2 mm).

The performance of the models was evaluated using several metrics such as Mean Absolute Error (MAE), Root Mean Squared Error (RMSE), Normalized RMSE (NRMSE), and Normalized MAE (NMAE). Both the Decision Tree (DT) and Random Forest (RF) models showed comparable performance for temperature (T) predictions, with an MAE of 4.04 and 4.46, respectively, and an RMSE of 26.6 and 28.7. The correlation coefficient for temperature predictions was 0.999 for DT and 0.998 for RF, indicating an excellent relationship between the predicted and actual values, while the R^2 scores were both 0.997, demonstrating a strong model fit.

For CH, both models achieved exceptionally low errors across all performance metrics, with MSE values of 2.53×10^{-12} for DT and 2.68×10^{-12} for RF. The MAE values were 1.20×10^{-7} for DT and 1.32×10^{-7} for RF, and the RMSE values were in the range of 1.59×10^{-6} and 1.64×10^{-6} . Both models achieved correlation coefficients around 0.929 and 0.922 for CH, with R^2 scores of 0.859 and 0.850, indicating a good model fit. For OH predictions, the models exhibited a slightly different performance. The RMSE values

were 7.25×10^{-5} for DT and 8.02×10^{-5} for RF, while the NRMSE values were 0.333 for DT and 0.369 for RF. The correlation coefficient for OH was 0.998 for DT and 0.997 for RF, suggesting high predictive accuracy, with R^2 values of 0.996 and 0.995, respectively. Notably, both models demonstrated strong overall performance, with some minor discrepancies. The combination of machine learning and DNS provides valuable insights into predicting ignition kernel growth and energy deposition dynamics. Both models performed well in predicting temperature and OH concentrations, with slightly higher errors in CH predictions.

For the analysis, both DT and RF models were employed to predict plasma-assisted ignition kernel growth, with a specific focus on temperature (T), CH, and OH species concentration at 100% energy deposition. The models were trained on datasets at 85%, 90%, and 115% energy deposition levels, and predictions were validated against a detailed DNS model. The performance metrics show a high degree of accuracy for both models but with some discrepancies.

7.1. Decision Tree Model (DT)

The DT model performed strongly, with an RMSE of 26.6 and an NRMSE of 0.0436 for temperature predictions, indicating excellent predictive accuracy. For CH and OH species concentrations, the DT model recorded RMSE values of 1.59×10^{-6} and 7.25×10^{-5} , respectively, indicating high precision. The MAE for the DT model was 4.04 for temperature and ranged from 1.20×10^{-7} to 7.14×10^{-6} for CH and OH, further confirming the model's robust predictions. The correlation coefficient was 0.999 for temperature, showing a near-perfect linear relationship between predicted and actual values.

7.2. Random Forest Model (RF)

The RF model exhibited a slightly higher error for temperature predictions, with an RMSE of 28.7 and an NRMSE of 0.0471. For CH, the RF model achieved minimal error, with an RMSE of 1.64×10^{-6} and zero error for certain metrics. The correlation coefficient for temperature predictions was 0.998, while for CH and OH, it was 0.922 and 0.997, respectively. The RF model displayed strong generalization, particularly around complex regions such as the ignition kernel edges, and performed similarly to the DT model, with minor variations in accuracy.

7.3. Comparative Analysis of DT and RF Models

A comparative analysis between the DT and RF models shows that both performed well in predicting the ignition kernel growth, especially for temperature. However, the RF model had a more uniform error distribution, making it slightly better at handling predictions in regions with rapid changes in temperature, such as at the edges of the ignition kernel. The DT model had lower RMSE and NRMSE values, indicating slightly better precision, but higher error concentrations were noted near the kernel edges, where the temperature gradients are more pronounced.

Both models demonstrated strong correlation coefficients and high R^2 values, with DT achieving 0.97 and RF showing similar results. The minimum absolute error for both models was 0.0, indicating that under certain conditions, the models provided perfect predictions. While the RF model had a marginally higher RMSE and NRMSE, it demonstrated better generalization across the kernel regions, which is particularly useful in predicting temperature distributions with complex dynamics.

In Figures 14–16, the spatio-temporal comparisons for temperature, OH, and CH patterns are displayed at three distinct time intervals (30 μ s, 40 μ s, and 50 μ s) using both Decision Tree (DT) and Random Forest (RF) models. Each figure provides critical insights into how these models perform at capturing combustion characteristics in a domain of 2 mm \times 2 mm. Figure 14 (Temperature Patterns) presents the temperature contours at three time steps. The visual patterns reflect the growth of the ignition kernel over time. Initially, a concentrated hot region forms, which expands outward as time progresses. Both

models capture the kernel expansion; however, slight differences between the DT and RF models can be observed in the smoothness and gradient transitions. The DT model displays slightly smoother temperature gradients compared to the RF model, especially at the kernel edges. This indicates that RF handles rapid temperature transitions with more uniformity, which is critical for predicting the growth of the ignition kernel accurately. The Decision Tree model has more error concentration at the edges where the temperature gradients are pronounced.

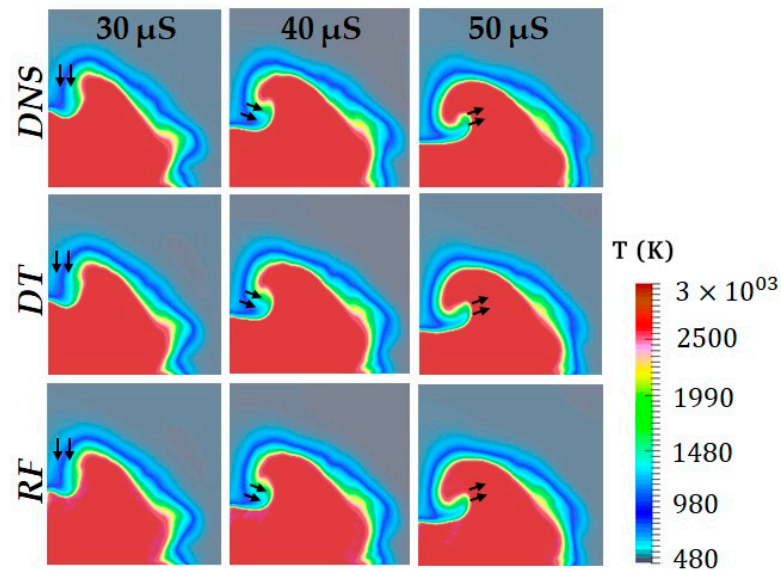


Figure 14. Comparison of spatio-temporal temperature patterns at 30 μ s, 40 μ s, and 50 μ s for DNS, Decision Tree (DT), and Random Forest (RF) models (Visualization area: 2 mm \times 2 mm).

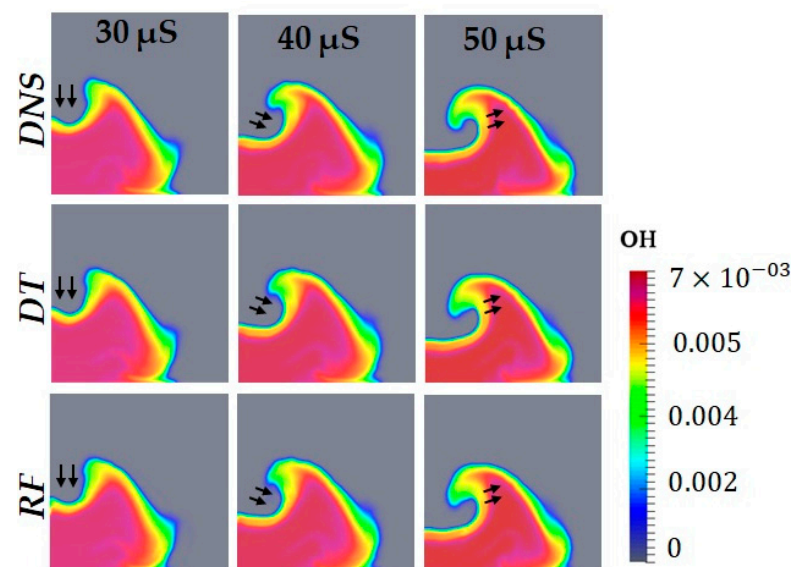


Figure 15. Comparison of spatio-temporal OH (mass fraction) patterns at 30 μ s, 40 μ s, and 50 μ s for DNS, Decision Tree (DT), and Random Forest (RF) models (Visualization area: 2 mm \times 2 mm).

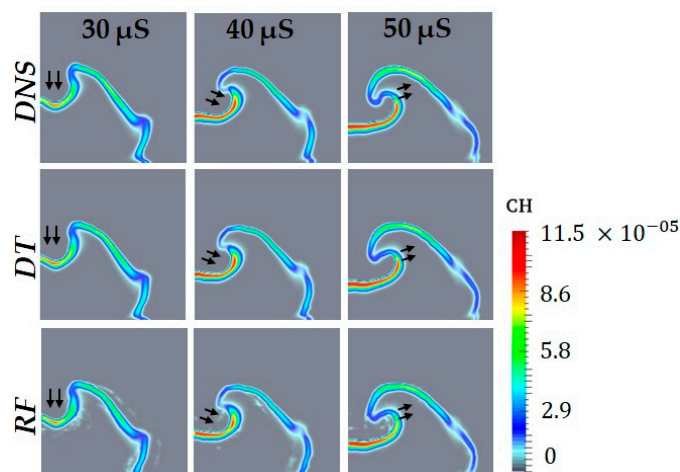


Figure 16. Comparison of spatio-temporal CH (mass fraction) patterns at 30 μ s, 40 μ s, and 50 μ s for DNS, Decision Tree (DT), and Random Forest (RF) models (Visualization area: 2 mm \times 2 mm).

Figure 15 (OH Patterns) depicts the distribution of OH radicals, a key marker for combustion, over time. The OH distribution reflects areas of active combustion, often surrounding the ignition kernel. The shape of these distributions varies slightly between DT and RF, with RF showing more evenly distributed OH concentrations. RF's ability to generalize across the kernel regions provides a better representation of OH distribution. While both models track the radical distribution, the RF model shows a better handling of rapid changes in OH concentration, an important aspect for modeling flame structure.

Figure 16 (CH Radical Patterns) distributions are presented at the same time intervals. Like the OH patterns, the CH contours help to identify key regions in the flame where intermediate combustion species are present. Both models show similar kernel growth, but there are slight variations in how each model tracks the spread and intensity of CH concentrations. As seen in the figure, the Decision Tree model has challenges in capturing the exact spread of CH compared to the RF model, with a more pronounced difference seen in the outer regions of the ignition kernel. This suggests that RF might be better at tracking species like CH under varying temperatures and combustion conditions, which is critical for accurately modeling flame chemistry.

In Figure 17, the performance of two machine learning models (DT and RF) is investigated, and their sensitivity is presented in comparison to the DNS model for predicting ignition-driven variables. The temperature comparison at different time scales, the points scatter around the perfect sensitivity line ($T_{ML} = T_{DNS}$), showing how closely the DT and RF models predict temperature compared to the DNS. In the low-temperature range (roughly 500 K to 1500 K in the periphery of the kernel), both the Decision Tree (DT, red dots) and Random Forest (RF, blue dots) predictions closely follow the perfect sensitivity line. This is the region of smooth temperature transitions, characterized by lower gradients and gradual curvature changes. This makes it easier for ML models to learn and make better predictions based on the training data. In this region, the models are likely encountering more linear or less complex relationships between the input features and temperature, making it easier for both DT and RF to generalize well. In the high-temperature range (above 2000 K), the predicted values from both models start to deviate significantly from the DNS values, with more scattered points away from the perfect sensitivity line. High-temperature regions typically correspond to the core region of the ignition kernel with a sharper temperature gradient making it difficult to train for the ML models. High-temperature regions may involve highly nonlinear processes, such as rapid chemical reactions, or changes in thermo-physical properties. These nonlinearities are harder for models like Decision Trees and even Random Forests to capture accurately.

Decision Trees are simple models that tend to overfit noisy data, especially in complex regions. Random Forests, being an ensemble of Decision Trees, help to reduce overfitting,

but they still may not capture all the intricate details of the high-temperature behavior. As RFs perform better than DTs at low-temperature regions but still struggle to accurately predict in the high-temperature region, this suggests that even though ensemble methods reduce variance and improve predictions, the complexity of the underlying phenomena at higher temperatures requires either more complex models or better data representation. Gradient boosting methods and deep learning models, such as Neural Networks, may more effectively capture the nonlinearities present in high-temperature regions compared to Decision Trees or Random Forests. Additionally, incorporating more relevant features or transforming existing ones could enhance the model's ability to represent nonlinear behavior, thereby improving prediction accuracy at elevated temperatures.

Figure 17 also compares the predictions of DT and RF for OH radical concentrations (OH_{ML}) against the true OH concentrations obtained from DNS at time steps of 30 μs , 40 μs , and 50 μs . Both models perform well in the low and high OH concentration regions but have difficulty accurately capture the behavior in the middle concentration range (0.002 to 0.005), where the data points are more scattered. At a low concentration region (0 to ~ 0.002), chemical reactions are relatively slow or in the quenching phase, making the system's dynamics simpler and more predictable. As a result, both models, particularly the DT, predict OH concentrations with high accuracy. The relationships between input features like temperature, pressure, and reaction rates are more straightforward and likely linear, which allows both models to learn and generalize well. At high OH concentrations region (above ~ 0.005), the chemical reactions may be approaching saturation or equilibrium, leading to more stable system behavior. This stabilization simplifies prediction tasks for both models, as OH concentrations change less drastically.

Consequently, both DT and RF show good agreement with DNS values, with Decision Tree often showing slightly better performance in this range. Accurate predictions at high OH concentrations are crucial because these regions are where active combustion occurs, and modeling OH radicals precisely is vital for understanding combustion efficiency and pollutant formation. The middle-concentration range (~ 0.002 to ~ 0.005 , Poorly Captured) exhibits more scatter and larger deviations from the perfect sensitivity line, indicating that both models struggle to capture the true behavior of the DNS data. This region represents a transitional phase between low and high OH concentrations, where the combustion process is highly dynamic, with rapid changes in OH radical concentrations. These nonlinear and complex interactions make it challenging for DT and RF to predict accurately. The transition is inherently difficult to model, especially with decision-based models, as they may fail to capture the nuances of these rapid changes.

In comparison, both models show good agreement with DNS data at low and high-concentration regions. Decision Tree consistently performs better than Random Forest, especially in the low and high-OH-concentration ranges, where its predictions are more tightly clustered around the ideal line. In contrast, Random Forest shows more scatter in the low-concentration range. The ability of Decision Tree to capture OH radical behavior more accurately at high concentrations highlights its effectiveness in modeling critical intermediates in combustion reactions. While both models provide good performance in stable regions, their limitations in the middle-concentration range suggest the need for more advanced approaches. To improve predictions in this region, more complex models, such as gradient boosting or Deep Neural Networks, which are better equipped to handle nonlinearities and dynamic interactions in combustion processes. Additionally, enhancing feature engineering by introducing inputs that better capture the behavior of OH radicals at mid concentrations, and including more training data in this range, could help improve model accuracy. In conclusion, while Decision Tree outperforms Random Forest in both low and high-OH-concentration ranges, both models could benefit from improvements in handling the mid-range nonlinearity to provide more accurate and reliable predictions across all regions of OH concentrations.

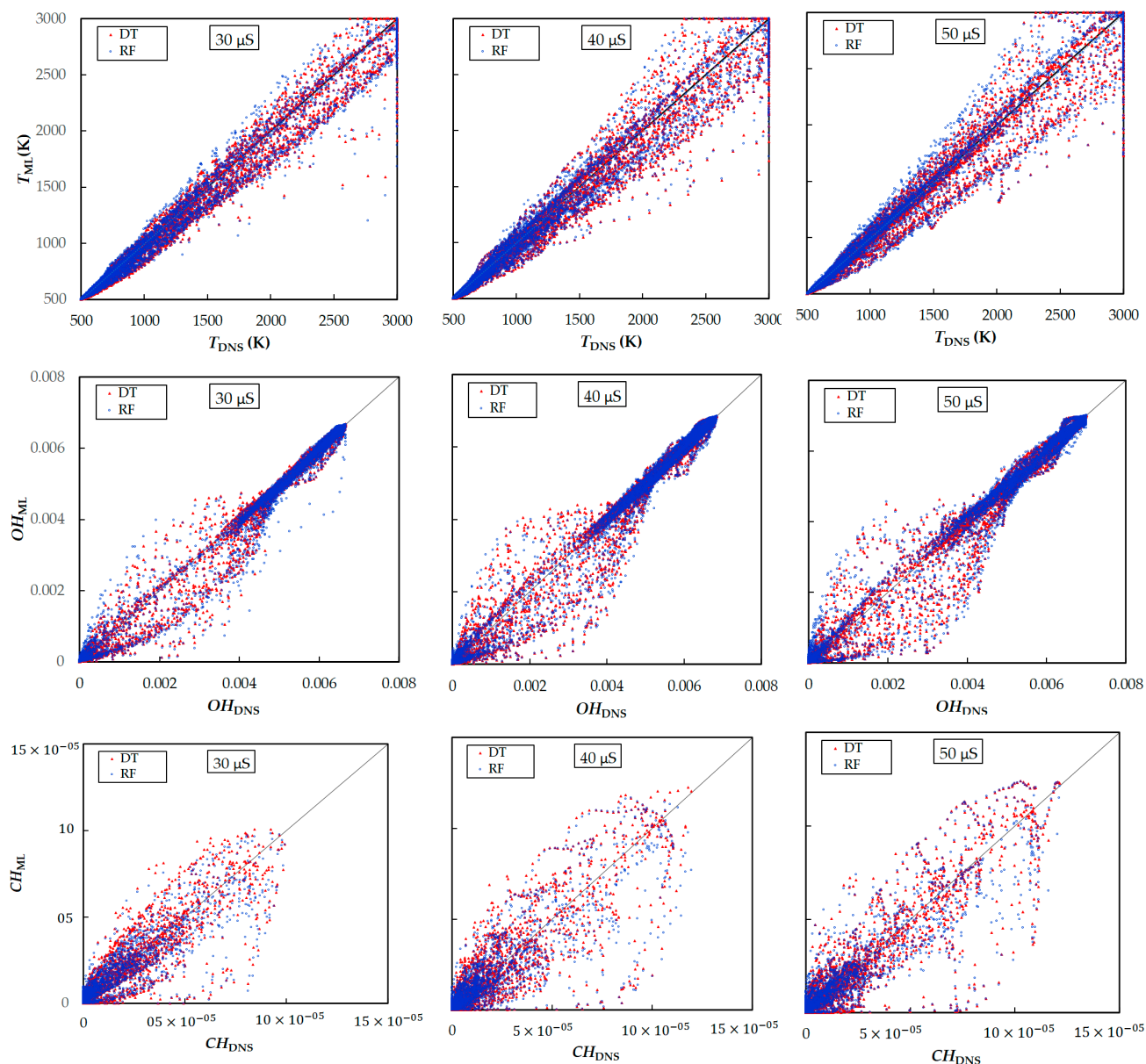


Figure 17. Sensitivity analysis of DNS vs. Decision Tree (DT) and Random Forest (RF) predictions for temperature, OH, and CH at 30, 40, and 50 μs .

To compare the CH radical concentrations (CH_{ML}) against the DNS values (CH_{DNS}) at time steps of 30 μs , 40 μs , and 50 μs , both models perform well in the low-concentration range (approximately 0 to 5×10^{-5}), closely matching the DNS data. However, at higher concentrations, both models show significant deviations from the DNS values. This makes it easier for both models, especially Random Forests, to generalize from the training data and capture the behavior of the system accurately. The stable behavior in this region allows the models to perform well without much complexity. One reason for the poor performance in this region could be an imbalanced training dataset. As a result, both Decision Trees and Random Forests deviate significantly from the true DNS values in the high-concentration range. Decision Trees are particularly prone to overfitting, which could cause them to capture the low-concentration region accurately while failing to model the complexities of higher concentrations, leading to significant errors. Although Random Forests mitigate overfitting by combining multiple Decision Trees, they may still underfit the more complex high-concentration data, resulting in reduced performance in this range. Both models may struggle to capture this behavior because they are trained on broader conditions that do

not adequately represent this specific phase of the reaction dynamics. To improve model performance in this range, more advanced machine learning techniques, such as deep learning or gradient boosting, and better training data representation should be considered to capture the nonlinearities, and intricate interactions present at higher CH concentrations.

8. Conclusions

Turbulent combustion plays a crucial role in various fields like energy production, aerospace, environmental processes, and industrial applications. It is a highly dynamic process involving complex interactions between chemical reactions and turbulent flow, which make the process immensely chaotic and very difficult to predict. Key challenges of turbulent combustion include resolving turbulent and chemical phenomena across a wide range of spatial and temporal scales, precisely capturing the multiscale, nonlinear interactions between turbulence and chemical kinetics, etc. Conventional modeling approaches attempt to approximate turbulence and combustion dynamics but are often computationally expensive and require simplifications that limit their accuracy. This is where machine learning offers transformative impact. The integration of machine learning into turbulent combustion modeling uses data-driven techniques that enhance the predictive accuracy of conventional models and significantly reduce computational costs. Table 4 illustrates the current scope of machine learning across various stages of combustion, encompassing ignition through flame propagation.

Table 4. Application of machine learning at different stages of combustion.

Combustion Stage	Machine Learning Techniques	Practical Implications	References
Ignition	Artificial Neural Networks (ANNs), Support Vector Machines (SVMs), Decision Tree (DT), and Random Forest (RF)	<ul style="list-style-type: none"> • Predict ignition delay • Optimize ignition conditions • Ignition kernel profile 	Molana et al. [142], Tuan et al. [146], Sharif et al. [23]
Flame Kernel Development	Decision Tree (DT), Random Forest (RF), and Convolutional Neural Network (CNN)	<ul style="list-style-type: none"> • Estimate flame kernel growth • Optimize fuel–air mixture 	Johnson et al. [147]
Transition to Turbulent Flame	Convolutional Neural Network Long Short-Term Memory (CNN-LSTM)	<ul style="list-style-type: none"> • Predict flame structure • Improve flame evolution modeling 	Ren et al. [25]
Flame–Turbulence Interaction	Neural Networks, SVMs, Physics-Informed Neural Networks (PINNs), Reinforced Learning	<ul style="list-style-type: none"> • Optimize combustion behavior • Capture flame turbulence interaction • Optimize flame stability 	Yan et al. [148], Li et al. [149]
Flame Propagation	Artificial Neural Networks (ANNs) and Convolutional Neural Network Long Short-Term Memory (CNN-LSTM)	<ul style="list-style-type: none"> • Predict flame speed • Improve combustion efficiency • Reduce emissions 	Sadeq et al. [150], Ren et al. [25]

Machine learning helps to identify key patterns in large combustion datasets, optimize turbulent flame behavior, and provide real-time predictions for complex interactions involved in turbulent combustion. At the ignition stage, techniques such as Neural Networks and Support Vector Machines (SVMs) are commonly used to predict ignition delays that help to optimize fuel efficiency and system reliability. Convolutional Neural Networks (CNNs), Decision Tree (DT), and Long Short-Term Memory (LSTM) models can provide predictions of flame growth and expansion to ensure efficient fuel–air mixture management. Neural Networks are effective for capturing the complex flame–turbulence interactions that allow better control over the flame dynamics. Convolutional Neural Networks and Artificial Neural Networks (ANNs) are useful techniques to approximate turbulent flame propagation for optimizing combustion efficiency and reducing emission. Thus, the application of machine learning techniques at different stages of turbulent combustion improves accuracy, increases efficiency, and optimizes the combustion dynamics.

This study also presented the results of machine learning methods, specifically DT and RF, for the spatio-temporal prediction of plasma-assisted ignition kernels in a stoichiometric methane/air mixture based on the initial degree of ionization. The findings demonstrated that well-trained machine learning models can accurately predict the spatio-temporal ignition kernel profile based on the initial energy deposition and distribution. The integration of machine learning in combustion simulation represents a promising interdisciplinary approach that can substantially enhance predictive capabilities and deepen our understanding of combustion phenomena. The simulation results of plasma-assisted ignition kernel growth, acquired from the presented models, support this assertion effectively.

Author Contributions: R.M. and M.P.S. conceptualized the work. R.M. and his graduate students, M.E.S. and S.M.Y.B., conducted the literature review section. S.M.Y.B. and R.M. contributed to the MLS-based ignition kernel training, testing, and analysis, as well as the ML-based plasma-assisted ignition kernel section. M.E.S., S.M.Y.B., M.P.S. and R.M. contributed to the revision. All authors have read and agreed to the published version of the manuscript.

Funding: The work was exploratory and was partially supported by the internal grant of Idaho State University.

Institutional Review Board Statement: Not applicable.

Data Availability Statement: All data generated or analyzed during this study are included in this submitted article. Data/experimental results are presented in the manuscript and, if appropriate, datasets/experimental results used and/or analyzed during the current study are available from the corresponding author on reasonable request.

Conflicts of Interest: The authors declare no conflict of interest.

Abbreviations

AI	Artificial Intelligence	ANN	Artificial Neural Network
CFD	Computational Fluid Dynamics	CH	Hydrocarbon
CMC	Conditional Moment Closure	CNN	Convolutional Neural Network
CPU	Central Processing Unit	DI	Direct Integration
DNN	Deep Neural Network	DNS	Direct Numerical Simulation
DRG	Directed Relation Graph	DT	Decision Tree
ECN	Engine Combustion Network	FGM	Flamelet-Generated Manifold
FPV	Flamelet Progress Variable	GPU	Graphics Processing Unit
HCCI	Homogeneous Charge Compression Ignition	ILDm	Intrinsic Low-Dimensional Manifolds
ISAT	In-Situ Adaptive Tabulation	KNN	K-Nearest Neighbors
LEM	Linear-Eddy Model	LES	Large-Eddy Simulation
LHS	Latin Hypercube Sampling	LSTM	Long Short-Term Memory
LUT	Look-Up Table	MAE	Mean Absolute Error
MDP	Markov Decision Process	ML	Machine Learning
MLP	Multilayer Perceptron	MMC	Multiple Mapping Conditioning
MoE	Mixture of Experts	NO _x	Nitrogen Oxide
ODE	Ordinary Differential Equation	ODT	One-Dimensional Turbulence
OH	Hydroxyl Radical	PCA	Principal Component Analysis
PDF	Probability Density Function	PFR	Plug-Flow Reactor
PIV	Particle Image Velocimetry	PLIF	Planar Laser-Induced Fluorescence
PaSR	Partially Stirred Reactor	QSSA	Quasi-Steady State Approximation
RAM	Random Access Memory	RANS	Reynolds-Averaged Navier–Stokes
RCCE	Rate-Controlled Constrained Equilibrium	RF	Random Forest
RL	Reinforcement Learning	RMSE	Root Mean Squared Error
RNN	Recurrent Neural Network	SOM	Self-Organizing Map
SO _x	Sulfur Oxide	SVM	Support Vector Machines
UFE	Unsteady Flame Embedding	UFPV	Unsteady Flamelet Progress Variable
UHC	Unburnt Hydrocarbon	VULCAN	Upwind Algorithm for Complex Flow Analysis

References

1. Kondratiev, V.N. Combustion. Encyclopedia Britannica. Available online: <https://www.britannica.com/science/combustion> (accessed on 24 September 2024).
2. Tyurenkova, V.; Smirnova, M. Material combustion in oxidant flows: Self-similar solutions. *Acta Astronaut.* **2016**, *120*, 129–137. [[CrossRef](#)]
3. Veynante, D.; Vervisch, L. Turbulent combustion modeling. *Prog. Energy Combust. Sci.* **2002**, *28*, 193–266. [[CrossRef](#)]
4. Betelin, V.; Nikitin, V.; Mikhilchenko, E. 3D numerical modeling of a cylindrical RDE with an inner body extending out of the nozzle. *Acta Astronaut.* **2020**, *176*, 628–646. [[CrossRef](#)]
5. Poludnenko, A.Y.; Gardiner, T.A.; Oran, E.S. Spontaneous Transition of Turbulent Flames to Detonations in Unconfined Media. *Phys. Rev. Lett.* **2011**, *107*, 054501. [[CrossRef](#)] [[PubMed](#)]
6. Tropina, A.A.; Mahamud, R. Effect of Plasma on the Deflagration to Detonation Transition. *Combust. Sci. Technol.* **2022**, *194*, 2752–2770. [[CrossRef](#)]
7. Tropina, A.; Mahamud, R.; Yorn, D.W.; Miles, R.B. Deflagration to detonation transition assisted by equilibrium and non-equilibrium plasma. In *AIAA Aviation 2019 Forum*; AIAA AVIATION Forum; American Institute of Aeronautics and Astronautics: Reston, VA, USA, 2019.
8. Cherif, M.A.; Masuda, R.; Claverie, A.; Starikovskaia, S.M.; Vidal, P. Plasma-enhanced detonability: Experimental and calculated reduction of the detonation cell size. *Combust. Flame* **2024**, *268*, 113639. [[CrossRef](#)]
9. Nikitin, V.; Mikhilchenko, E. Safety of a rotating detonation engine fed by acetylene–oxygen mixture launching stage. *Acta Astronaut.* **2022**, *194*, 496–503. [[CrossRef](#)]
10. Williams, F. *Combustion Theory*; Addison-Wesley: Boston, MA, USA, 1985.
11. Tyurenkova, V.V.; Stamov, L.I. Flame propagation in weightlessness above the burning surface of material. *Acta Astronaut.* **2019**, *159*, 342–348. [[CrossRef](#)]
12. Kushnirenko, A.; Stamov, L.; Tyurenkova, V.; Smirnova, M.; Mikhilchenko, E. Three-dimensional numerical modeling of a rocket engine with solid fuel. *Acta Astronaut.* **2021**, *181*, 544–551. [[CrossRef](#)]
13. Lackner, M.; Palotás, Á.; Winter, F. *Combustion: From Basics to Applications*, 1st ed.; Wiley-VCH: Weinheim, Germany, 2013.
14. Kennedy, L.A. *Turbulent Combustion*; American Institute of Aeronautics and Astronautics: Reston, VA, USA, 1978.
15. Barwey, S.; Hassanaly, M.; Raman, V.; Steinberg, A. Using Machine Learning to Construct Velocity Fields from OH-PLIF Images. *Combust. Sci. Technol.* **2022**, *194*, 93–116. [[CrossRef](#)]
16. Zhang, Y.; Zhang, D.; Jiang, H. Review of Challenges and Opportunities in Turbulence Modeling: A Comparative Analysis of Data-Driven Machine Learning Approaches. *J. Mar. Sci. Eng.* **2023**, *11*, 1440. [[CrossRef](#)]
17. Pitsch, H. Large-eddy simulation of turbulent combustion. *Annu. Rev. Fluid Mech.* **2006**, *38*, 453–482. [[CrossRef](#)]
18. Vervisch, L.; Hauguel, R.; Domingo, P.; Rullaud, M. Three facets of turbulent combustion modelling: DNS of premixed V-flame, LES of lifted nonpremixed flame and RANS of jet-flame. *J. Turbul.* **2004**, *5*, 004. [[CrossRef](#)]
19. Gicquel, L.Y.; Staffelbach, G.; Poinso, T. Large eddy simulations of gaseous flames in gas turbine combustion chambers. *Prog. Energy Combust. Sci.* **2012**, *38*, 782–817. [[CrossRef](#)]
20. Nikitin, V.; Karandashev, I.; Malsagov, M.Y.; Mikhilchenko, E. Approach to combustion calculation using neural network. *Acta Astronaut.* **2022**, *194*, 376–382. [[CrossRef](#)]
21. Mal’sagov, M.Y.; Mikhil’chenko, E.V.; Karandashev, I.; Nikitin, V.F. Simulation of hydrogen combustion at different pressures using a neural network. *Combust. Explos. Shock Waves* **2023**, *59*, 145–150. [[CrossRef](#)]
22. An, J.; Wang, H.; Liu, B.; Luo, K.H.; Qin, F.; He, G.Q. A deep learning framework for hydrogen-fueled turbulent combustion simulation. *Int. J. Hydrogen Energy* **2020**, *45*, 17992–18000. [[CrossRef](#)]
23. Bhuiyan, S.M.Y.; Mostafa, T.; Schoen, M.P.; Mahamud, R. Assessment of Machine Learning Approaches for the Predictive Modeling of Plasma-Assisted Ignition Karnal Growth. In Proceedings of the ASME, International Mechanical Engineering Congress and Exposition, Portland, OR, USA, 17–21 November 2024.
24. Peters, N. Turbulent combustion. *Meas. Sci. Technol.* **2001**, *12*, 2022. [[CrossRef](#)]
25. Ren, J.; Wang, H.; Chen, G.; Luo, K.; Fan, J. Predictive models for flame evolution using machine learning: A priori assessment in turbulent flames without and with mean shear. *Phys. Fluids* **2021**, *33*, 055113. [[CrossRef](#)]
26. Yao, S.; Wang, B.; Kronenburg, A.; Stein, O. Modeling of sub-grid conditional mixing statistics in turbulent sprays using machine learning methods. *Phys. Fluids* **2020**, *32*, 115124. [[CrossRef](#)]
27. Seltz, A.; Domingo, P.; Vervisch, L.; Nikolaou, Z.M. Direct mapping from LES resolved scales to filtered-flame generated manifolds using convolutional neural networks. *Combust. Flame* **2019**, *210*, 71–82. [[CrossRef](#)]
28. El-Nabulsi, R.A.; Anukool, W. Modeling of combustion and turbulent jet diffusion flames in fractal dimensions. *Contin. Mech. Thermodyn.* **2022**, *34*, 1219–1235. [[CrossRef](#)]
29. Blurock, E.; Battin-Leclerc, F. Modeling combustion with detailed kinetic mechanisms. In *Cleaner Combustion: Developing Detailed Chemical Kinetic Models*; Springer: Berlin/Heidelberg, Germany, 2013; pp. 17–57.
30. Eigentler, F.; Gerlinger, P. A detailed PAH and soot model for complex fuels in CFD applications. *Flow Turbul. Combust.* **2022**, *109*, 225–251. [[CrossRef](#)]
31. Law, C.K. Combustion in two-phase flows. In *Combustion Physics*; Cambridge University Press: Cambridge, UK, 2006; pp. 559–633.

32. Warnatz, J.; Maas, U.; Dibble, R.W. Combustion of liquid and solid fuels. In *Combustion: Physical and Chemical Fundamentals, Modeling and Simulation, Experiments, Pollutant Formation*; Springer: Berlin/Heidelberg, Germany, 2006; pp. 239–258.
33. Sakurai, A.; Maruyama, S.; Matsubara, K.; Miura, T.; Behnia, M. An efficient method for radiative heat transfer applied to a turbulent channel flow. *J. Heat Transf.* **2010**, *132*, 1–7. [[CrossRef](#)]
34. Paul, S.C.; Paul, M.C. Radiative heat transfer during turbulent combustion process. *Int. Commun. Heat Mass Transf.* **2010**, *37*, 1–6. [[CrossRef](#)]
35. Viskanta, R. Radiative transfer in turbulent flames. In *Thermopedia*; Begel House Inc.: Danbury, CT, USA, 2011.
36. De, S.; Agarwal, A.K.; Chaudhuri, S.; Sen, S. *Modeling and Simulation of Turbulent Combustion*; Springer: Berlin/Heidelberg, Germany, 2018.
37. Ge, H.-W.; Zhu, M.-M.; Chen, Y.-L.; Gutheil, E. Hybrid unsteady RANS and PDF method for turbulent non-reactive and reactive flows. *Flow Turbul. Combust.* **2007**, *78*, 91–109. [[CrossRef](#)]
38. Da Ronch, A.; Panzeri, M.; Drofelnik, J.; d'Ippolito, R. Sensitivity and calibration of turbulence model in the presence of epistemic uncertainties. *CEAS Aeronaut. J.* **2020**, *11*, 33–47. [[CrossRef](#)]
39. Echehki, T.; Mastorakos, E. *Turbulent Combustion Modeling: Advances, New Trends and Perspectives*; Springer: Berlin/Heidelberg, Germany, 2010.
40. Bilger, R. Turbulent jet diffusion flames. In *Energy and Combustion Science*; Elsevier: Amsterdam, The Netherlands, 1979; pp. 109–131.
41. Saha, A. Spatio-Temporal Analysis of Highly Dynamic Flows. Ph.D. Thesis, Purdue University Graduate School, West Lafayette, IN, USA, 2023.
42. Libby, P.; Williams, F. Fundamental aspects. In *Turbulent Reacting Flows*; Springer: Berlin/Heidelberg, Germany, 2005; pp. 1–43.
43. Salunkhe, A.; Deighan, D.; DesJardin, P.E.; Chandola, V. Physics informed machine learning for chemistry tabulation. *J. Comput. Sci.* **2023**, *69*, 102001. [[CrossRef](#)]
44. Shrivastava, S.; Gohel, S.; Srinivasa, M.; Patil, H.; Nakod, P. Accuracy Improvement of Flamelet Generated Manifold (FGM) Model in Modeling Partially Premixed Combustion Systems by Combining Machine Learning. In Proceedings of the ASME 2023 Gas Turbine India Conference, Bangalore, India, 7–8 December 2023.
45. Bilger, R. Conditional moment closure for turbulent reacting flow. *Phys. Fluids A Fluid Dyn.* **1993**, *5*, 436–444. [[CrossRef](#)]
46. de Frahan, M.T.H.; Yellapantula, S.; King, R.; Day, M.S.; Grout, R.W. Deep learning for presumed probability density function models. *Combust. Flame* **2019**, *208*, 436–450. [[CrossRef](#)]
47. Bishop, C.M.; Nasrabadi, N.M. *Pattern Recognition and Machine Learning*; Springer: Berlin/Heidelberg, Germany, 2006; Volume 4.
48. Klimenko, A.Y.; Pope, S.B. The modeling of turbulent reactive flows based on multiple mapping conditioning. *Phys. Fluids* **2003**, *15*, 1907–1925. [[CrossRef](#)]
49. Cleary, M.; Klimenko, A.Y. Multiple mapping conditioning: A new modelling framework for turbulent combustion. In *Turbulent Combustion Modeling: Advances, New Trends and Perspectives*; Springer: Berlin/Heidelberg, Germany, 2011; pp. 143–173.
50. Kerstein, A.R. Linear-eddy modelling of turbulent transport. Part 6. Microstructure of diffusive scalar mixing fields. *J. Fluid Mech.* **1991**, *231*, 361–394. [[CrossRef](#)]
51. Sen, B.A.; Menon, S. Linear eddy mixing based tabulation and artificial neural networks for large eddy simulations of turbulent flames. *Combust. Flame* **2010**, *157*, 62–74. [[CrossRef](#)]
52. Ranjan, R.; Panchal, A.; Karpe, S.; Menon, S. Machine Learning Strategy for Subgrid Modeling of Turbulent Combustion Using Linear Eddy Mixing Based Tabulation. In *Machine Learning and Its Application to Reacting Flows: ML and Combustion*; Springer International Publishing: Cham, Switzerland, 2023; pp. 175–208.
53. Kerstein, A.R. One-dimensional turbulence: Model formulation and application to homogeneous turbulence, shear flows, and buoyant stratified flows. *J. Fluid Mech.* **1999**, *392*, 277–334. [[CrossRef](#)]
54. Sutherland, J.C.; Punati, N.; Kerstein, A.R. *A Unified Approach to the Various Formulations of the One-Dimensional Turbulence Model*; University of Utah, Institute for Clean and Secure Energy: Salt Lake City, UT, USA, 2010.
55. Schmidt, R.C.; Kerstein, A.R.; McDermott, R. ODTLES: A multi-scale model for 3D turbulent flow based on one-dimensional turbulence modeling. *Comput. Methods Appl. Mech. Eng.* **2010**, *199*, 865–880. [[CrossRef](#)]
56. El-Asrag, H.A.; Ghoniem, A.F. Unsteady Flame Embedding. In *Turbulent Combustion Modeling: Advances, New Trends and Perspectives*; Springer: Berlin/Heidelberg, Germany, 2011; pp. 277–300.
57. El-Asrag, H.; Nave, J.-C.; Ghoniem, A. Unsteady flame embedding (UFE) subgrid model for turbulent premixed combustion simulations. In Proceedings of the 48th AIAA Aerospace Sciences Meeting Including the New Horizons Forum and Aerospace Exposition, Orlando, FL, USA, 4–7 January 2010; p. 201.
58. Vasilev, I.; Slater, D.; Spacagna, G.; Roelants, P.; Zocca, V. *Python Deep Learning: Exploring Deep Learning Techniques and Neural Network Architectures with Pytorch, Keras, and TensorFlow*; Packt Publishing Ltd.: Birmingham, UK, 2019.
59. Kalogirou, S.A. Artificial intelligence for the modeling and control of combustion processes: A review. *Prog. Energy Combust. Sci.* **2003**, *29*, 515–566. [[CrossRef](#)]
60. Pulga, L.; Bianchi, G.; Falfari, S.; Forte, C. A machine learning methodology for improving the accuracy of laminar flame simulations with reduced chemical kinetics mechanisms. *Combust. Flame* **2020**, *216*, 72–81. [[CrossRef](#)]
61. Shabaniyan, S.R.; Edrisi, S.; Khoram, F.V. Prediction and optimization of hydrogen yield and energy conversion efficiency in a non-catalytic filtration combustion reactor for jet A and butanol fuels. *Korean J. Chem. Eng.* **2017**, *34*, 2188–2197. [[CrossRef](#)]

62. Janakiraman, V.M. Machine Learning for Identification and Optimal Control of Advanced Automotive Engines. Ph.D. Thesis, University of Michigan, Ann Arbor, MI, USA, 2013.
63. Petzold, L.; Zhu, W. Model reduction for chemical kinetics: An optimization approach. *AIChE J.* **1999**, *45*, 869–886. [[CrossRef](#)]
64. Zhou, L.; Song, Y.; Ji, W.; Wei, H. Machine learning for combustion. *Energy AI* **2022**, *7*, 100128. [[CrossRef](#)]
65. Aliramezani, M.; Koch, C.R.; Shahbakhti, M. Modeling, diagnostics, optimization, and control of internal combustion engines via modern machine learning techniques: A review and future directions. *Prog. Energy Combust. Sci.* **2022**, *88*, 100967. [[CrossRef](#)]
66. Takbiri-Borujeni, A.; Ayoobi, M. Application of physics-based machine learning in combustion modeling. In Proceedings of the 11th US National Combustion Meeting, Pasadena, CA, USA, 24–27 March 2019.
67. Alipour, E.; Akhtardanesh, M.; Malaek, S. Application of Machine Learning to Bring Efficiency to Costly Experiments; Case of Flame-Extinction. *Fuel Combust.* **2024**, *17*, 20–36.
68. Malpica Galassi, R.; Ciottoli, P.P.; Valorani, M.; Im, H.G. Local combustion regime identification using machine learning. *Combust. Theory Model.* **2022**, *26*, 135–151. [[CrossRef](#)]
69. Brunton, S.L.; Noack, B.R.; Koumoutsakos, P. Machine Learning for Fluid Mechanics. *Annu. Rev. Fluid Mech.* **2020**, *52*, 477–508. [[CrossRef](#)]
70. Nasteski, V. An overview of the supervised machine learning methods. *Horizons B* **2017**, *4*, 56. [[CrossRef](#)]
71. Kotsiantis, S.B.; Zaharakis, I.; Pintelas, P. Supervised machine learning: A review of classification techniques. *Emerg. Artif. Intell. Appl. Comput. Eng.* **2007**, *160*, 3–24.
72. Duraisamy, K.; Iaccarino, G.; Xiao, H. Turbulence modeling in the age of data. *Annu. Rev. Fluid Mech.* **2019**, *51*, 357–377. [[CrossRef](#)]
73. Aghbashlo, M.; Peng, W.; Tabatabaei, M.; Kalogirou, S.A.; Soltanian, S.; Hosseinzadeh-Bandbafha, H.; Mahian, O.; Lam, S.S. Machine learning technology in biodiesel research: A review. *Prog. Energy Combust. Sci.* **2021**, *85*, 100904. [[CrossRef](#)]
74. Srinivas, S.; Babu, R.V. Deep learning in neural networks: An overview. *Comput. Sci.* **2015**, *61*, 85–117.
75. Lapeyre, C.J.; Misdariis, A.; Cazard, N.; Veynante, D.; Poinso, T. Training convolutional neural networks to estimate turbulent sub-grid scale reaction rates. *Combust. Flame* **2019**, *203*, 255–264. [[CrossRef](#)]
76. Huang, J.; Liu, H.; Cai, W. Online in situ prediction of 3-D flame evolution from its history 2-D projections via deep learning. *J. Fluid Mech.* **2019**, *875*, R2. [[CrossRef](#)]
77. Usama, M.; Qadir, J.; Raza, A.; Arif, H.; Yau, K.-L.A.; Elkhatib, Y.; Hussain, A.; Al-Fuqaha, A. Unsupervised machine learning for networking: Techniques, applications and research challenges. *IEEE Access* **2019**, *7*, 65579–65615. [[CrossRef](#)]
78. Dike, H.U.; Zhou, Y.; Deverasetty, K.K.; Wu, Q. Unsupervised learning based on artificial neural network: A review. In Proceedings of the 2018 IEEE International Conference on Cyborg and Bionic Systems (CBS), Shenzhen, China, 25–27 October 2018; pp. 322–327.
79. Kaiser, E.; Noack, B.R.; Cordier, L.; Spohn, A.; Segond, M.; Abel, M.; Daviller, G.; Öst, J.; Krajnović, S.; Niven, R.K. Cluster-based reduced-order modelling of a mixing layer. *J. Fluid Mech.* **2014**, *754*, 365–414. [[CrossRef](#)]
80. Kohonen, T. Essentials of the self-organizing map. *Neural Netw.* **2013**, *37*, 52–65. [[CrossRef](#)]
81. Moisy, F.; Jiménez, J. Geometry and clustering of intense structures in isotropic turbulence. *J. Fluid Mech.* **2004**, *513*, 111–133. [[CrossRef](#)]
82. He, G.; Jin, G.; Yang, Y. Space-time correlations and dynamic coupling in turbulent flows. *Annu. Rev. Fluid Mech.* **2017**, *49*, 51–70. [[CrossRef](#)]
83. Wiering, M.A.; Van Otterlo, M. Reinforcement learning. *Adapt. Learn. Optim.* **2012**, *12*, 729.
84. Li, Y. Deep reinforcement learning: An overview. *arXiv* **2017**, arXiv:1701.07274.
85. Si, J.; Wang, G.; Li, P.; Mi, J. Optimization of the global reaction mechanism for MILD combustion of methane using artificial neural network. *Energy Fuels* **2020**, *34*, 3805–3815. [[CrossRef](#)]
86. Ghraieb, H.; Viquerat, J.; Larcher, A.; Meliga, P.; Hachem, E. Single-step deep reinforcement learning for open-loop control of laminar and turbulent flows. *Phys. Rev. Fluids* **2021**, *6*, 053902. [[CrossRef](#)]
87. Swazinna, P.; Udluft, S.; Hein, D.; Runkler, T. Comparing model-free and model-based algorithms for offline reinforcement learning. *IFAC-PapersOnLine* **2022**, *55*, 19–26. [[CrossRef](#)]
88. Garg, P.; Silvas, E.; Willems, F. Potential of machine learning methods for robust performance and efficient engine control development. *IFAC-PapersOnLine* **2021**, *54*, 189–195. [[CrossRef](#)]
89. Cheng, Y.; Huang, Y.; Pang, B.; Zhang, W. ThermalNet: A deep reinforcement learning-based combustion optimization system for coal-fired boiler. *Eng. Appl. Artif. Intell.* **2018**, *74*, 303–311. [[CrossRef](#)]
90. Lamont, W.G.; Roa, M.; Lucht, R.P. Application of artificial neural networks for the prediction of pollutant emissions and outlet temperature in a fuel-staged gas turbine combustion rig. In Proceedings of the Turbo Expo: Power for Land, Sea, and Air, Düsseldorf, Germany, 16–20 June 2014.
91. Ding, T.; Readshaw, T.; Rigopoulos, S.; Jones, W.P. Machine learning tabulation of thermochemistry in turbulent combustion: An approach based on hybrid flamelet/random data and multiple multilayer perceptrons. *Combust. Flame* **2021**, *231*, 111493. [[CrossRef](#)]
92. Ge, Y.; Cleary, M.J.; Klimenko, A.Y. A comparative study of Sandia flame series (D–F) using sparse-Lagrangian MMC modelling. *Proc. Combust. Inst.* **2013**, *34*, 1325–1332. [[CrossRef](#)]

93. Garmory, A.; Mastorakos, E. Capturing localised extinction in Sandia Flame F with LES–CMC. *Proc. Combust. Inst.* **2011**, *33*, 1673–1680. [[CrossRef](#)]
94. Jones, W.P.; Prasad, V.N. Large Eddy Simulation of the Sandia Flame Series (D–F) using the Eulerian stochastic field method. *Combust. Flame* **2010**, *157*, 1621–1636. [[CrossRef](#)]
95. Chu, H.; Xiang, L.; Nie, X.; Ya, Y.; Gu, M.; E, J. Laminar burning velocity and pollutant emissions of the gasoline components and its surrogate fuels: A review. *Fuel* **2020**, *269*, 117451. [[CrossRef](#)]
96. Freund, J.; Sirignano, J.; MacArt, J. *Machine-Learning Turbulence Models for Simulations of Turbulent Combustion*; Blue Waters Annual Report; NCSA—National Center for Supercomputing Applications: Chicago, IL, USA, 2019; pp. 148–149.
97. Meyer, R.; Schmuck, K.S.; Hauser, A.W. Machine learning in computational chemistry: An evaluation of method performance for nudged elastic band calculations. *J. Chem. Theory Comput.* **2019**, *15*, 6513–6523. [[CrossRef](#)]
98. Roncancio, R.; El Gamal, A.; Gore, J.P. Turbulent flame image classification using Convolutional Neural Networks. *Energy AI* **2022**, *10*, 100193. [[CrossRef](#)]
99. Seltz, A. Application of Deep Learning to Turbulent Combustion Modeling of Real Jet Fuel for the Numerical Prediction of Particulate Emissions. Ph.D. Thesis, Normandie Université, Normandy, France, 2020.
100. Gitushi, K.M.; Ranade, R.; Echehki, T. Investigation of deep learning methods for efficient high-fidelity simulations in turbulent combustion. *Combust. Flame* **2022**, *236*, 111814. [[CrossRef](#)]
101. An, J.; He, G.; Luo, K.; Qin, F.; Liu, B. Artificial neural network based chemical mechanisms for computationally efficient modeling of hydrogen/carbon monoxide/kerosene combustion. *Int. J. Hydrogen Energy* **2020**, *45*, 29594–29605. [[CrossRef](#)]
102. Font, B.; Weymouth, G.D.; Nguyen, V.-T.; Tutty, O.R. Deep learning of the spanwise-averaged Navier–Stokes equations. *J. Comput. Phys.* **2021**, *434*, 110199. [[CrossRef](#)]
103. Roncancio, R.; Kim, J.; El Gamal, A.; Gore, J.P. Data-driven Analysis of Turbulent Flame Images. In Proceedings of the AIAA Scitech 2021 Forum, Virtual Event, 11–15 and 19–21 January 2021.
104. Lee, M.; Yoon, S.; Kim, J.; Wang, Y.; Lee, K.; Park, F.C.; Sohn, C.H. Classification of impinging jet flames using convolutional neural network with transfer learning. *J. Mech. Sci. Technol.* **2022**, *36*, 1547–1556. [[CrossRef](#)]
105. Shamsudheen, F.A.; Yalamanchi, K.; Yoo, K.H.; Voice, A.; Boehman, A.; Sarathy, M. Machine Learning Techniques for Classification of Combustion Events under Homogeneous Charge Compression Ignition (HCCI) Conditions. *SAE Int.* **2020**. [[CrossRef](#)]
106. Gobyzov, O.A.; Tokarev, M.P.; Abdurakipov, S.S.; Lobasov, A.S. Flame state diagnostics using visualization and neural network analysis. *AIP Conf. Proc.* **2018**, *2027*, 040067.
107. Nguyen, H.-T.; Domingo, P.; Vervisch, L.; Nguyen, P.-D. Machine learning for integrating combustion chemistry in numerical simulations. *Energy AI* **2021**, *5*, 100082. [[CrossRef](#)]
108. Wan, K.; Barnaud, C.; Vervisch, L.; Domingo, P. Chemistry reduction using machine learning trained from non-premixed micro-mixing modeling: Application to DNS of a syngas turbulent oxy-flame with side-wall effects. *Combust. Flame* **2020**, *220*, 119–129. [[CrossRef](#)]
109. Chen, J.Y.; Kollmann, W.; Dibble, R.W. Pdf Modeling of Turbulent Nonpremixed Methane Jet Flames. *Combust. Sci. Technol.* **1989**, *64*, 315–346. [[CrossRef](#)]
110. Maas, U.; Pope, S.B. Implementation of simplified chemical kinetics based on intrinsic low-dimensional manifolds. *Symp. (Int.) Combust.* **1992**, *24*, 103–112. [[CrossRef](#)]
111. Pope, S.B. Computationally efficient implementation of combustion chemistry using in situ adaptive tabulation. *Combust. Theory Model.* **1997**, *1*, 41–63. [[CrossRef](#)]
112. Christo, F.; Masri, A.; Nebot, E.; Turányi, T. Utilising artificial neural network and repro-modelling in turbulent combustion. In Proceedings of the ICNN'95-International Conference on Neural Networks, Perth, WA, Australia, 27 November–1 December 1995; pp. 911–916.
113. Christo, F.C.; Masri, A.R.; Nebot, E.M. Artificial neural network implementation of chemistry with pdf simulation of H₂/CO₂ flames. *Combust. Flame* **1996**, *106*, 406–427. [[CrossRef](#)]
114. Christo, F.C.; Masri, A.R.; Nebot, E.M.; Pope, S.B. An integrated PDF/neural network approach for simulating turbulent reacting systems. *Symp. (Int.) Combust.* **1996**, *26*, 43–48. [[CrossRef](#)]
115. Chen, J.Y.; Blasco, J.A.; Fueyo, N.; Dopazo, C. An economical strategy for storage of chemical kinetics: Fitting in situ adaptive tabulation with artificial neural networks. *Proc. Combust. Inst.* **2000**, *28*, 115–121. [[CrossRef](#)]
116. Blasco, J.; Fueyo, N.; Dopazo, C.; Chen, J.-Y. A self-organizing-map approach to chemistry representation in combustion applications. *Combust. Theory Model.* **2000**, *4*, 61–76. [[CrossRef](#)]
117. Chatzopoulos, A.K.; Rigopoulos, S. A chemistry tabulation approach via Rate-Controlled Constrained Equilibrium (RCCE) and Artificial Neural Networks (ANNs), with application to turbulent non-premixed CH₄/H₂/N₂ flames. *Proc. Combust. Inst.* **2013**, *34*, 1465–1473. [[CrossRef](#)]
118. Franke, L.L.C.; Chatzopoulos, A.K.; Rigopoulos, S. Tabulation of combustion chemistry via Artificial Neural Networks (ANNs): Methodology and application to LES-PDF simulation of Sydney flame L. *Combust. Flame* **2017**, *185*, 245–260. [[CrossRef](#)]
119. Demir, S.; Kundu, P.; Owoyele, O. Implementation of high dimensional flamelet manifolds for supersonic combustion using deep neural networks. In Proceedings of the AIAA Aviation 2020 Forum, Virtual Event, 15–19 June 2020; p. 3059.
120. Terrapon, V.; Ham, F.; Pecnik, R.; Pitsch, H. A flamelet-based model for supersonic combustion. *Annu. Res. Briefs* **2009**, 47–58.

121. Berglund, M.; Fureby, C. LES of supersonic combustion in a scramjet engine model. *Proc. Combust. Inst.* **2007**, *31*, 2497–2504. [[CrossRef](#)]
122. Oevermann, M. Numerical investigation of turbulent hydrogen combustion in a SCRAMJET using flamelet modeling. *Aerosp. Sci. Technol.* **2000**, *4*, 463–480. [[CrossRef](#)]
123. Saghafian, A.; Terrapon, V.E.; Pitsch, H. An efficient flamelet-based combustion model for compressible flows. *Combust. Flame* **2015**, *162*, 652–667. [[CrossRef](#)]
124. Saghafian, A.; Shunn, L.; Philips, D.A.; Ham, F. Large eddy simulations of the HIFiRE scramjet using a compressible flamelet/progress variable approach. *Proc. Combust. Inst.* **2015**, *35*, 2163–2172. [[CrossRef](#)]
125. Quinlan, J.; Drozda, T.G.; McDaniel, J.C.; Lacaze, G.; Oefelein, J.C. A priori analysis of a compressible flamelet model using RANS data for a dual-mode scramjet combustor. In Proceedings of the 22nd AIAA Computational Fluid Dynamics Conference, Dallas, TX, USA, 22–26 June 2015; p. 3208.
126. Quinlan, J. Flamelet/Progress Variable Modeling for a Dual-Mode Scramjet Combustor. Ph.D. Thesis, University of Virginia, Charlottesville, VA, USA, 2015.
127. Drozda, T.G.; Quinlan, J.R.; Drummond, J.P. Flamelet modeling for supersonic combustion. *Model. Simul. Turbul. Mix. React. Power Energy Flight* **2020**, 127–168.
128. Ladeinde, F.; Lou, Z. Improved flamelet modeling of supersonic combustion. *J. Propuls. Power* **2018**, *34*, 750–761. [[CrossRef](#)]
129. Ladeinde, F.; Lou, Z.; Li, W. The effects of pressure treatment on the flamelet modeling of supersonic combustion. *Combust. Flame* **2019**, *204*, 414–429. [[CrossRef](#)]
130. Aspden, A.J.; Day, M.S.; Bell, J.B. Turbulence–flame interactions in lean premixed hydrogen: Transition to the distributed burning regime. *J. Fluid Mech.* **2011**, *680*, 287–320. [[CrossRef](#)]
131. Gruber, A.; Chen, J.H.; Valiev, D.; Law, C.K. Direct numerical simulation of premixed flame boundary layer flashback in turbulent channel flow. *J. Fluid Mech.* **2012**, *709*, 516–542. [[CrossRef](#)]
132. Wang, H.; Hawkes, E.R.; Chen, J.H. Turbulence–flame interactions in DNS of a laboratory high Karlovitz premixed turbulent jet flame. *Phys. Fluids* **2016**, *28*, 095107. [[CrossRef](#)]
133. Wang, H.; Hawkes, E.R.; Chen, J.H. A direct numerical simulation study of flame structure and stabilization of an experimental high Ka CH₄/air premixed jet flame. *Combust. Flame* **2017**, *180*, 110–123. [[CrossRef](#)]
134. Wang, H.; Hawkes, E.R.; Zhou, B.; Chen, J.H.; Li, Z.; Aldén, M. A comparison between direct numerical simulation and experiment of the turbulent burning velocity-related statistics in a turbulent methane–air premixed jet flame at high Karlovitz number. *Proc. Combust. Inst.* **2017**, *36*, 2045–2053. [[CrossRef](#)]
135. Ronneberger, O.; Fischer, P.; Brox, T. U-net: Convolutional networks for biomedical image segmentation. In Proceedings of the Medical Image Computing and Computer-Assisted Intervention–MICCAI 2015: 18th International Conference, Munich, Germany, 5–9 October 2015; Proceedings; Proceedings, Part III 18. pp. 234–241.
136. Owoyele, O.; Nunno, A.C.; Pal, P.; Kundu, P. Unsteady Flamelet/Progress Variable Modeling of Spray Flames with Mixture of Experts-Based Representation of Combustion Manifold. In Proceedings of the LES for Energy Conversion in Electric and Combustion Engines Conference, Virtual, 16–18 June 2021.
137. Owoyele, O.; Nunno, A.C.; Pal, P.; Kundu, P. Flamelet modeling of spray flames with mixture of experts-based learning of combustion manifolds. In Proceedings of the 2nd International Conference on Energy and AI, London, UK, 9–13 August 2021.
138. Kempf, A.; Flemming, F.; Janicka, J. Investigation of lengthscales, scalar dissipation, and flame orientation in a piloted diffusion flame by LES. *Proc. Combust. Inst.* **2005**, *30*, 557–565. [[CrossRef](#)]
139. Ihme, M.; Schmitt, C.; Pitsch, H. Optimal artificial neural networks and tabulation methods for chemistry representation in LES of a bluff-body swirl-stabilized flame. *Proc. Combust. Inst.* **2009**, *32*, 1527–1535. [[CrossRef](#)]
140. Hansinger, M.; Ge, Y.; Pfitzner, M. Deep Residual Networks for Flamelet/progress Variable Tabulation with Application to a Piloted Flame with Inhomogeneous Inlet. *Combust. Sci. Technol.* **2022**, *194*, 1587–1613. [[CrossRef](#)]
141. Prieler, R.; Moser, M.; Eckart, S.; Krause, H.; Hochenauer, C. Machine learning techniques to predict the flame state, temperature and species concentrations in counter-flow diffusion flames operated with CH₄/CO/H₂–air mixtures. *Fuel* **2022**, *326*, 124915. [[CrossRef](#)]
142. Molana, M.; Darougheh, S.; Biglar, A.; Chamkha, A.J.; Zoldak, P. Machine Learning Approaches for Predicting Ignition Delay in Combustion Processes: A Comprehensive Review. *Ind. Eng. Chem. Res.* **2024**, *63*, 2509–2518. [[CrossRef](#)]
143. Mahamud, R.; Tropina, A.A.; Shneider, M.N.; Miles, R.B. Dual-pulse laser ignition model. *Phys. Fluids* **2018**, *30*, 106104. [[CrossRef](#)]
144. Mahamud, R. Mechanism of nonequilibrium plasma-enhanced ignition in the event of dual-pulse laser energy deposition. *J. Phys. D Appl. Phys.* **2022**, *55*, 435201. [[CrossRef](#)]
145. Smirnov, N.N.; Betelin, V.B.; Nikitin, V.F.; Stamov, L.I.; Altoukhov, D.I. Accumulation of errors in numerical simulations of chemically reacting gas dynamics. *Acta Astronaut.* **2015**, *117*, 338–355. [[CrossRef](#)]
146. Tuan, N.V.; Minh, D.Q.; Khoa, N.X.; Lim, O. A Study to Predict Ignition Delay of an Engine Using Diesel and Biodiesel Fuel Based on the ANN and SVM Machine Learning Methods. *Acs Omega* **2023**, *8*, 9995–10005. [[CrossRef](#)]
147. Johnson, R.; Kaczynski, D.; Zeng, W.; Warey, A.; Grover, R.; Keum, S. *Prediction of Combustion Phasing Using Deep Convolutional Neural Networks*; SAE Technical Paper; SAE International: Warrendale, PA, USA, 2020; ISSN 0148-7191.
148. Yan, P.; Cao, Z.; Peng, J.; Yang, C.; Yu, X.; Qiu, P.; Zhang, S.; Han, M.; Liu, W.; Jiang, Z. A Neural Network-Based Flame Structure Feature Extraction Method for the Lean Blowout Recognition. *Aerospace* **2024**, *11*, 57. [[CrossRef](#)]

149. Li, K.; Savari, C.; Sheikh, H.A.; Barigou, M. A data-driven machine learning framework for modeling of turbulent mixing flows. *Phys. Fluids* **2023**, *35*, 015150. [[CrossRef](#)]
150. Sadeq, A.M.; Moghaddam, A.H.; Sleiti, A.K.; Ahmed, S.F. Development of Machine Learning Models for Studying the Premixed Turbulent Combustion of Gas-To-Liquids (GTL) Fuel Blends. *Korean J. Chem. Eng.* **2024**, *41*, 479–494. [[CrossRef](#)]

Disclaimer/Publisher’s Note: The statements, opinions and data contained in all publications are solely those of the individual author(s) and contributor(s) and not of MDPI and/or the editor(s). MDPI and/or the editor(s) disclaim responsibility for any injury to people or property resulting from any ideas, methods, instructions or products referred to in the content.